

Predicting Soil Salinity Using Machine Learning and Assessing Farmers' Adaptive Capacity: A Study in the Red River Delta

Farmers' adaptive capacity towards soil salinity effects using hybrid machine learning in the Red River Delta

Huu Duy Nguyen¹, Dinh Kha Dang², Thi Anh Tam Lai¹, Duc Dung Tran³, Himan Shahabi⁴, Quang-Thanh Bui¹

¹ Faculty of Geography, VNU University of Science, Vietnam National University, Ha Noi, 334 Nguyen Trai, Thanh Xuan district, Hanoi City, Vietnam; nguyenhuuduy@hus.edu.vn; laithianhtam_t65@hus.edu.vn; thanhbq@vnu.edu.vn

² Faculty of Hydrology, Meteorology, and Oceanography, VNU University of Science, Vietnam National University, Ha Noi, 334 Nguyen Trai, Thanh Xuan district, Hanoi, Vietnam; dangdinhkha@hus.edu.vn

³ National Institute of Education, Nanyang Technological University, Singapore, Singapore; ⁴ Earth Observatory of Singapore and Asian School of the Environment, Nanyang Technological University, Singapore, Singapore; ⁵ Center of Water Management and Climate Change, Institute for Environment and Resources, Vietnam National University, Ho Chi Minh City, Viet Nam; dungtranducvn@yahoo.com

⁴ Departments of Geomorphology, Faculty of Natural Resources, University of Kurdistan, Sanandaj City, Kurdistan Province, Iran; h.shahabi@uok.ac.ir

Corresponding: Huu Duy Nguyen (nguyenhuuduy@hus.edu.vn)

Abstract

Soil salinity is a grave environmental threat to agricultural development and food security in large parts of the world, especially in the situation of global warming and sea level rise. Reliable information on the adaptive capacity of farms plays a key role in reducing the socioeconomic effects of soil salinization and helps policymakers and farmers propose more appropriate measures to combat the phenomenon. The ~~aim of the research~~ research aims is to design a theoretical framework to assess soil salinity and farmers' adaptive capacity, based on machine learning, optimization algorithms (namely, Xgboost (XGB), XGB–Pelican Optimization Algorithm (POA), XGB–Siberian Tiger Optimization (STO), XGB–Serval Optimization Algorithm (SOA), XGB–Particle Swarm Optimization (PSO), and XGB–Grasshopper Optimization Algorithm (GOA)), remote sensing, and interviews with local people. We evaluated the geographical distribution of soil salinity by applying machine learning to Sentinel 1 and 2A. ~~The geographical distribution of soil salinity was evaluated by applying machine learning Sentinel 1 and 2A.~~ The

Formatted: English (United States)

Formatted: English (United States)

adaptive capacity of farmers was evaluated through interviews with 87 households. The statistical indices, namely the mean absolute error (MAE), the root mean square error (RMSE), and the correlation coefficient (R^2), were used to assess the machine learning models. The outcome of this study demonstrated that all optimization algorithms were successful in improving the accuracy of the XGB model. The XGB-POA ~~was had~~ the most performance, with an R^2 value of 0.968, followed by XGB-STO ($R^2=0.967$), XGB-SOA ($R^2=0.966$), XGB-PSO ($R^2 = 0.964$), and XGB-GOA ($R^2=0.964$), respectively. The soil salinity map produced by the proposed models also indicated that the coastal and riverside regions were the most affected by soil salinity. The results also showed human and financial resources to be the two most important factors influencing the adaptive capacity of farmers. This study ~~offers~~ ~~provides~~ a key theoretical framework that ~~supplements the enhances previous~~ previous studies and can ~~support assist~~ policy-makers and farmers in ~~managing~~ land resource ~~management, for examplesuch as~~ accurately identifying areas affected by soil salinity for agricultural development in the context of climate change. In addition, this research highlights the importance of integrating machine learning, remote sensing, and socio-economic surveys in soil salinity management, which can support farmers for sustainable agricultural development.

Keywords: Red river, soil salinity, machine learning, adaptive capacity

1. Introduction

Soil salinity is among the greatest threats to land management, ~~poses-posing~~ significant problems to agricultural progress and global food security (He et al., 2024; Jia et al., 2024; Xiao et al., 2024). ~~According to FAO, soil salinity affects about 424 million hectares of land surface (with a depth of 0-30 cm)According to FAO, about 424 million hectares of land surface (with a depth of 0-30 cm)~~ and more than 833 million hectares of subsoil (30-100 cm) ~~are touched by soil salinity~~. This area is increasing by about 2 million hectares each year and influences more than 100 countries worldwide, causing damage between 12 and 27.3 billion USD (Aksoy et al., 2024; Jia et al., 2024).

The soil salinity problem will occur at the local, regional, and global levels (Bandak et al., 2024; Liu et al., 2024). In Vietnam, many littoral regions ~~are~~ affected by soil salinity problems. According to the 2021 Ministry of Agriculture and ~~Rural Development~~Environmental Report on the Current Situation and Planning of Agricultural Development, in 2020, about 200,000 hectares of cropland in Vietnam ~~were touched~~ ~~were already affected~~ by soil salinity. ~~The Red River and Mekong Deltas are~~ ~~This problem is increasingly serious in Mekong Delta and Red River Delta - home to more than~~ ~~over~~ 40 million people and ~~represent an extremely key role~~ ~~playing a key role~~ in Vietnam's agricultural and

Formatted: English (United States)

Formatted: English (United States)

Formatted: English (United States)

Formatted: English (United States)

Formatted: English (United States)

~~aquaculture sector~~the country's agricultural and aquaculture activities. ~~- where They they~~ account for 71% of paddy cultivation, 86% of aquatic farming, and 65% of fruit production (General Statistics Office, 2024; Ministry of Aquaculture, Agriculture and Rural Development, 2013). ~~Because T~~these low-lying coastal areas (Hung and Larson, 2014) are experiencing subsidence (Le Dang et al., 2014), ~~and declining river water levels, and river water levels are decreasing. As such, they are very~~have become highly susceptible to the effects of climate variability ~~and sea-level rise~~ (Dasgupta et al., 2009). ~~Soil salinization in the littoral regions of these two deltas partly due to the advance of the sea is becoming a major threat to crop production while also putting pressure on Vietnam's food abundance.~~ Therefore, monitoring soil salinity is essential to inform agricultural management strategies to ensure food security at local and regional levels.

In order to address the problem, it is important to have the most precise and current data on soil salinity. Traditionally, ~~direct field measurements of soil salinity yielded the most accurate data~~the most accurate data would ~~be obtained by measuring soil salinity directly in the field~~ (Eldeiry et al., 2008; Rhoades and Ingvalson, 1971). This method collects point samples in the areas of interest one by one, which is time-consuming and requires significant manual work. Although this method can accurately identify soil salinity, ~~there is no way for these data to be updated over time without conducting further field missions. To obtain a continuous math function, i.e., raster data suitable for GIS analysis and remote sensing for the areas of interest, freely accessible remote sensing data, such as those obtained via Landsat and Sentinel imagery, can monitor the environment with different spectral bands, at high spatial (10 m) and temporal (3 to 5 days) resolutions it requires so many field missions to collect the data over time, which can be time-consuming and resource-intensive. To reduce these limitations and obtain continuous spatial data~~ (such as raster data) suitable for GIS analysis and environmental monitoring, several studies have used freely available remote sensing data, such as Landsat and Sentinel images. These data provide spatial (10m) and temporal (3 to 5 days) resolution and capture multiple spectral bands (Asfaw et al., 2018; Cullu, 2003). ~~Remote sensing data has been justified by several studies by the ability to monitor soil salinity with high accuracy and faster. This process can be achieved by analyzing the relationships between remote sensing data and in situ data, provided these data are spatially and temporally consistent. Several studies have demonstrated the effectiveness of remote sensing to monitor soil salinity accurately and rapidly. By constructing correlations between remote sensing-derived indices and soil salinity points in the field, such as NDVI, VSSI, and NDSI, we can achieve this. Although remote sensing can monitor soil salinity using different spectral responses, slightly or moderately saline soils cannot be distinguished~~

Formatted: English (United States)

Formatted: English (United States)

Formatted: English (United States)

85 easily because soil minerals and their components modify the spectral capacity of the soil surface. To emphasize the
86 qualities of the land surface, for example, water, vegetation, or saline soil, several studies have highlighted indices
87 such as NDVI, VSSI, and NDSI to monitor soil salinity. Using an index with different wavebands increases the
88 number of variables in the soil salinity modelling process. Although remote sensing can monitor soil salinity using
89 different spectral responses, slightly or moderately saline soils cannot be distinguished easily because soil minerals
90 and their components modify the spectral capacity of the soil surface.

91 ~~In recent years~~ Recently, with improvements in computing power, machine learning, and deep learning, ~~there has~~
92 ~~been~~ ~~have greatly provided the~~ substantial growth ~~of in~~ techniques to construct soil salinity maps with higher
93 accuracy. Algorithms such as random forest (Fathizad et al., 2020), XGBoost (Jia et al., 2024), support vector
94 machines (Jiang et al., 2019), CatBoost (Gong et al., 2023; Wang et al., 2022), and AdaBoost (Wang et al., 2022)
95 are the most popular algorithms to construct soil salinity maps by integrating satellite images and in situ
96 measurements. Some research has used deep learning models to construct soil salinity maps, such as deep neural
97 networks, recurrent neural networks, and Deep Boltzmann machines. ~~(Kaplan et al., (2023) used four machine~~
98 learning algorithms, namely M5P, RF, Linear, and IBK, integrated with Sentinel 2A data and 393 soil samples
99 collected in situ to construct a soil salinity map for the United Arab Emirates. The study's ~~outcome results~~
100 ~~indicated~~ showed that all models' ~~accuracy was performed~~ well in assessing soil salinity, with the IBK model ~~proving~~
101 ~~demonstrating the most effective~~ highest effectiveness. ~~(Aksoy et al., (2024) used XGBoost and random forest with~~
102 26 environmental covariates from Landsat 8 OLI to evaluate soil salinity in Iran's Lake Urmia. The study's outcome
103 showed that machine learning integrated with Landsat 8 OLI data successfully monitored soil salinity, with XGB
104 yielding more accurate results than random forest. ~~(Jia et al., (2024) applied nine models, namely PLSR, Lasso,~~
105 CART, RF, ERT, GBDT, LightGBM, XGBoost, and AdaBoost, integrated with Sentinel 2A imagery, to evaluate
106 soil salinity in the Ningxia Yellow River Diversion Irrigation Area. The results showed that the AdaBoost model
107 performed better than the others.

108 Previous studies show that although machine learning methods have been utilized to assess soil salinity in many
109 regions of the world, their application for this purpose is still limited in the Mekong and Red River Deltas (Shi et al.,
110 2021; Vermeulen and Van Niekerk, 2017). Currently, there are only four studies that have assessed soil salinity in
111 the Mekong Delta (Hoa et al., 2019; Nguyen et al., 2023; Nguyen et al., 2018; Nguyen et al., 2021), and no work has

Field Code Changed

Field Code Changed

Field Code Changed

112 been done in this field for the Red River Delta. In addition, most previous studies have developed state-of-the-art
113 methods, such as integrating machine learning and remote sensing, to identify the geographical distribution of soil
114 salinity in different regions of the world (Hardie and Doyle, 2012; Su et al., 2020; Wang et al., 2007). While several
115 studies have highlighted the importance of assessing the adaptation capacity of the community to strengthen their
116 resilience to soil salinity and other types of natural hazards, however, very few studies integrate this aspect into the
117 identification of spatial soil salinity. Few studies have integrated the identification of the geographical distribution of
118 soil salinity with the adaptive capacity of farms. Several studies have, however, highlighted the importance of
119 measuring such adaptive capacity to improve the resilience of farms against soil salinization in particular and natural
120 hazards in general. (Hoang et al., (2023) reported that assessing the ability of farms to adapt to soil salinization is the
121 key to reducing vulnerability and contributes significantly to the development of sustainable livelihoods.

Formatted: English (United States)

Formatted: English (United States)

122 The adaptive capacity is defined as the capability of the community to cope, adjust, and adapt to the impacts of
123 growing soil salinity. It measures the ability to predict, respond, and recover from the phenomenon. It is assessed on
124 different scales, using different approaches, according to the region in question (Mazumder and Kabir, 2022; Thiam
125 et al., 2024). The IPCC in 2014 indicated that farm adaptive capacity depends on five main factors: natural capital,
126 human capital, material resources, financial resources, and social capital. Furthermore, understanding the adaptive
127 capacity of communities plays an important role in reducing the negative effects of salinity intrusion in coastal
128 regions in general and the Red River Delta in particular. By assessing adaptation at multiple scales with site-specific
129 methods, researchers and local governments can identify interventions (such as crop variety changes, crop calendars,
130 irrigation systems) that are effective. The IPCC in 2014 indicated that farm adaptive capacity depends on five main
131 factors: natural capital, human capital, material resources, financial resources, and social capital. Therefore,
132 integrating the adaptive capacity of populations with the soil salinity map improves the accuracy of predictions and
133 proposes adaptation strategies that strengthen the overall resilience of communities.

Formatted: English (United States)

Formatted: English (United States)

Formatted: English (United States)

134 The research aims to improve a theoretical framework to assess soil salinity and farmers' adaptive capacity based on
135 machine learning, optimization algorithms (namely XGB, XGB- POA, XGB- STO, XGB- SOA, XGB- PSO, and
136 XGB- GOA), remote sensing, and interviews with local people. This study used machine learning to construct the
137 soil salinity map. From the literature reviews, Several studies have been conducted in different regions of the
138 world, focusing on the adaptive ability of farmers examined farmer's adaptive capacity to environmental stressors in

139 different regions (Bhuyan et al., 2024; Thiam et al., 2024). However, no studies comprehensively analyze farmers'
140 adaptive ability to combat soil salinity in a given region based on machine learning, remote sensing, and interviews
141 with local people. In addition, several studies combine machine learning with Sentinel 1 or Sentinel 2 to assess soil
142 salinity (Wang et al., 2021; Xiao et al., 2023); however, there are rarely studies that combine machine learning with
143 Sentinel 1 and Sentinel 2 to monitor soil salinity in the Red River Delta. ~~Several studies have pointed out that~~ By the
144 combination of Sentinel 1 and Sentinel 2, advanced machine learning, and the information from farmers themselves,
145 this study filled a critical gap and provided a novel, comprehensive framework for monitoring and responding to soil
146 salinity in the Red River Delta~~the combination of Sentinel 1 and Sentinel 2 can reduce the limitations of each image,~~
147 ~~which can improve the accuracy of soil salinity monitoring in the context of climate change~~ (Ma et al., 2021).

148 In general, salinity intrusion harms agricultural development and people's livelihoods. Therefore, it is necessary to
149 develop a theoretical framework to address the soil salinity problem in terms of natural and social factors. However,
150 previous studies have mainly assessed the spatial distribution of salinity or the community's adaptive capacity, and
151 hardly any studies have assessed both the spatial distribution of salinity and the community's adaptive capacity.
152 Thus, the global contribution of this study is to fill the knowledge gap about the spatial distribution of soil salinity
153 and the adaptive capacity of communities in the Red River Delta in general and Thai Binh Province in particular by
154 relying on modern methods to improve this important and understudied understanding. The results of this study can
155 play an important role in mitigating the impact of salinity intrusion on agricultural development and can help
156 policymakers and planners develop effective strategies to mitigate this impact, especially in the context of climate
157 change.

Formatted: Vietnamese

158 ~~This map gives us a panoramic picture of the saline intrusion situation in the Thai Thuy district in particular and the~~
159 ~~Red River Delta region in general. This map will be the basis for identifying areas affected by saline intrusion,~~
160 ~~thereby assessing people's adaptability to this situation. The results of this study can inform farmers of developing~~
161 ~~strategies to reduce the impacts of soil salinity on agriculture and ensure food security in the region. To our~~
162 ~~knowledge, this study is considered the first study to assess the soil salinity and farmer's adaptive capacity of the~~
163 ~~population based on machine learning, remote sensing and interviews with the local people. The finding of this~~
164 ~~paper provides important information for policymakers or local authorities based on evidence and, ultimately,~~
165 ~~supports researchers or decision makers in developing effective strategies for smallholder farmers.~~

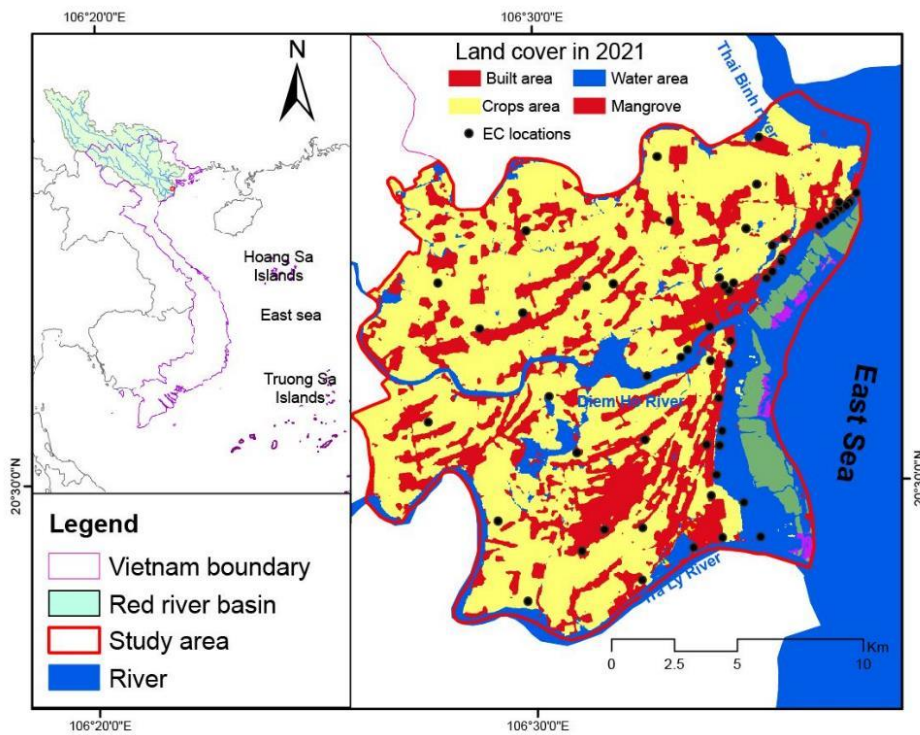
2. Study Area

The Red River Basin covers a total area of 169,000 km² and spans China (48%), Laos (0.7%), and Vietnam (51.3%). The river system has a total length of 1,150 km, with around 500 km in the territory of Vietnam before discharging into the Gulf of Tonkin. The topography is mainly mountainous terrain that comprises about 70% of the total area at elevations above 500 meters. In the lowlands, elevations range from approximately 0.4 to 9 m, ~~with the~~ characterized by a tropical climate with summer monsoons from the south and winter monsoons from the northeast (Vinh et al., 2014), the basin experiences average annual precipitation ranging from 800 to 3000 mm. The rainy season occurs from May to October and ~~registers-accounts~~ for 70%-90% of annual rainfall (Quang et al., 2024). Daily rainfall varies from 300-400 mm during this period. The average temperature ranges from 22 to 27 °C, with winter temperatures potentially below 10 °C and summer temperatures above ~~up~~ to 40 °C.

The basin flows into the Gulf of Tonkin through nine river mouths, of which the Tra Ly, Van Uc, and Ba Lat are the main channels for water conveyance. These channels transport a substantial sediment load of approximately 120×10⁶ tons annually to the Red River Delta region (Vinh et al., 2014). The littoral region has a semi-diurnal tidal regime, with tidal ranges ranging from 2 to 4 m. Saline intrusion significantly influences the littoral region during the dry season with average and maximum wave heights of about 0.7-1.3 m and 3.5-4.5 m, respectively. However, during major storms, wave heights can ~~obtained-at reach~~ 5 m (Nhuan et al., 2007).

The Red River Delta is influenced by several natural hazards, such as flooding, soil salinity, and sea level rise (Castelletti et al., 2012). Several studies have highlighted that rising sea levels are having an increasingly severe impact on inland regions, leading to soil salinity (Nguyễn Văn Đào, 2023). ~~In recent years~~ Recently, the Red River Delta in general and the Thai Thuy district in particular have been affected by soil salinity, causing significant damage to agricultural development and negatively impacting residents' livelihoods (Figure 1). According to the FAO report, if the sea level rises by 50 cm, about 11.8% of coastal land is at risk of being flooded by salt water; this figure increases to about 31.4% if the sea level rises by 100 cm in Thai Binh province. Recently, saltwater intrusion has clearly affected agricultural production in Thai Binh province and Thai Thuy district. Typically, in the 2015-2016 winter-spring crop, the salinity in the main rivers exceeded the threshold of 1‰, causing significant damage to crops. In 2020, the salinity in the main rivers, 28 km from the sea, exceeded the threshold of 3.75‰, far exceeding the allowable threshold of 2.75‰. This phenomenon greatly affects agricultural production in the area.

Formatted: Vietnamese



Formatted: Centered

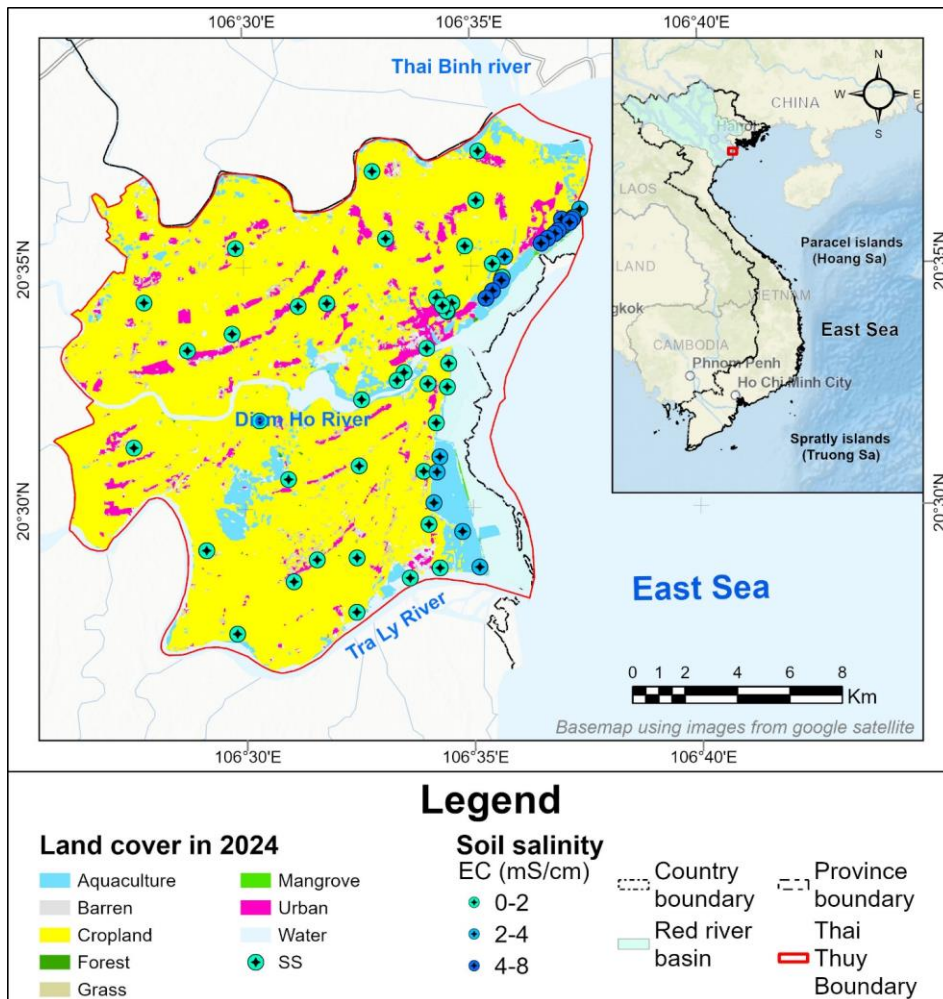


Figure 1: Geographical location of study area: The red boundary on the map represents the Thai Thuy district, located in the Thai Binh province in the Red River Delta of Vietnam. The green points are the soil salinity samples collected in April 2024. The land use in the Thai Thuy district is divided into eight types: aquaculture, barren land, cropland, forest, grass, mangrove, urban, and water body. While the aquaculture area is located in the coastal zone, cropland takes up a large part of the study area, and Urban is located in the center and along the road.

200 3. Methodology

201 The first strand of the methodology was the identification of the soil salinity mapping. ~~We divided this process into~~
202 ~~four main steps~~ ~~This process was divided into four main steps~~ (Figure 2):

203 Preparation of soil salinity samples and factors

204 The data for constructing the soil salinity map were divided into two main types: EC and conditioning factors.

205 *EC Measurements*

206 ~~We collected soil salinity samples using soil drills, employing both zigzag and grid techniques. Small-scale~~
207 ~~sampling frequently uses this technique~~ ~~Soil salinity samples were collected using soil drills using both zigzag and~~
208 ~~grid techniques. This technique is utilized frequently in small scale sampling~~ (Elshevy et al., 2024; Jia et al., 2024).

209 The sampling depth depends on the soil salinity assessment for each specific crop. This study monitors soil salinity
210 with the objective of agricultural development; therefore, soil samples were obtained from a ~~profoundness depth~~ of 0
211 to 30 cm. The sampling process occurred in the dry season, between March and April 2024. In addition, when
212 sampling in the field, it is necessary to consider the homogeneity of the soil. ~~We collected 62 samples to cover the~~
213 ~~entire field~~ ~~62 samples were collected to ensure coverage of the entire field.~~ ~~We collected samples along the road to~~
214 ~~identify different types of soil, and the farmers labeled the samples accordingly.~~ ~~Samples were collected along the~~
215 ~~road to get the different types of soil, and the farmers indicated samples.~~ The samples were locked in bags until
216 analysis in the laboratory. ~~We noted the positions of the samples, including longitude and latitude, during the~~
217 ~~sampling process. When the samples were sent to labs, they were stored in enameled jars, and impurities like stones,~~
218 ~~wood, and branches were removed~~ ~~The information on the positions of the samples, such as longitude and latitude,~~
219 ~~was noted in the sampling process. It should be noted that when the samples were transferred to laboratories, they~~
220 ~~were stored in enameled jars, and the impurities present in the samples, such as stones, wood, and branches, were~~
221 ~~removed.~~ These soil samples were then finely ground. The electrical conductivity (EC) was then calculated from a
222 1:5 soil/deionised water suspension. A soil/water suspension was created by adding 7 g of soil to 35 ml of distilled
223 water and then mixed with a mechanical stirrer for 60 minutes to dissolve the salt. The EC value was measured
224 using a conductivity probe. Finally, the samples were split into two parts: the first part (70%) was used to build the
225 proposed models, while the other part (30%) was applied to confirm the model.

226 Remote Sensing Data

227 Due to the effects of the earth's cycle, the salt accumulated in the soil is closely linked to climatic conditions,
228 hydrology, soil characteristics, and surface vegetation density, for example, topographic characteristics (Wang et al.,
229 2024; Xie et al.). ~~We calculated these factors using optical Sentinel 2A images and microwave Sentinel 1 images to~~
230 ~~determine the soil salinity value. These factors were calculated using the optical Sentinel 2A images and microwave~~
231 ~~Sentinel 1 images to identify the soil salinity value.~~ The Sentinel-2A images were calculated by running Sen2Cor for
232 atmospheric correction to ensure the transition between apparent atmospheric reflectance and surface reflectance,
233 and these images were obtained using Google Earth Engine. To reduce the influence of clouds, Sentinel 2A images
234 for March-April 2024 were selected with a cloud cover rate of less than 10%. To enhance the quality of these
235 images, the median value of each pixel was calculated at a resolution of 10 m. As for the Sentinel 1 images, they
236 were acquired in dual cross-polarization mode and broadband interferometric mode. The median value of the
237 Sentinel 1 image obtained on March 31, 2024, was computed to acquire microwave remote sensing data at a scale of
238 10 m. As well as 12 bands of the Sentinel 2A image (from band 1 to band 12) and 3 indices of the Sentinel 1 image
239 (VV, VH, and VVHH). In addition, 20 spectral indices ~~extracted from Sentinel 2A image~~~~extraits à partir de~~
240 ~~l'image Sentinel 2A~~ were selected to build the soil salinity model, namely Brightness index (BI), Canopy Response
241 Salinity Index (CRSI), Enhanced Vegetation Index (EVI), Intensity index 1 (Int1), Intensity index 2 (Int2),
242 Normalized Difference Salinity Index (NDSI), Normalized Difference Vegetation Index (NDVI), Ratio Vegetation
243 Index (RVI), Salinity index (S1), Salinity index (S2), Salinity index (S3), Salinity index (S5), Salinity index (S6),
244 Soil Adjusted Vegetation Index (SAVI), Salinity Index 1 (SI), Salinity index 2 (SI1), Salinity index 3 (SI2), Salinity
245 index 4 (SI3) and Salinity index 5 (SI4). These factors were divided into three main groups: vegetation indices
246 (NDVI, CRSI, RVI, SAVI, and EVI), water indices (flow direction and distance to river), salinity indices (SI, SI1,
247 SI2, SI3, SI4, S1, S2, S3, S5, S6, and NDSI), topography indices (elevation and slope), and chlorophyll spectral
248 indices (BI, Int1, Int2). These indices have been used frequently in previous studies (Hoa et al., 2019; Nguyen et al.,
249 2021; Wang et al., 2021).

250 The indices due to the vegetation reflect the health and growth of vegetation, and ~~the present study~~~~This~~ indirectly
251 reflects the level of soil salinity in any region. The increase in soil salinity has a negative effect on the development
252 of vegetation due to the difference in the absorption of water and nutrients; therefore, it leads to a decrease in the

values of NDVI, RVI, SAVI, and EVI and an increase in the value of CRSI_ (Jia et al., 2024; Wang et al., 2024).

Water indices play an important role because regions near rivers or along the flow path are more affected by the salinity risk. River flow is often affected by tides or seawater intrusion; therefore, when the distance to the river decreases, the salinity risk increases due to the infiltration of salty river water into the soil. Furthermore, the flow direction influences the propagation and infiltration of water in the soil. Salty water can penetrate further inland if the flow is from the sea to the river, especially in the dry season (Nguyen et al., 2021).

Topography indices are key in constructing soil salinity models, as salty water penetrates low-lying regions more easily. In the Red River Delta, the low-lying regions are located along the coastline, and as such, these regions are more affected by the risk of soil salinity. Salinity indices highlight the value of spectral reflectance in regions affected by saltwater intrusion. The higher the salinity, the higher the spectral reflectance value (Du et al., 2024).

Construction of hybrid machine learning models

~~We built six machine-learning models to identify the spatial distribution of soil salinity. Six machine-learning models were built to identify the spatial distribution of soil salinity.~~ This involved two main steps: constructing an individual XGB model and then creating hybrid models by integrating each of five optimization algorithms with the XGB model. ~~We developed the XGB model using Python and the Sklearn library. The XGB model was developed using Python and the Sklearn library. Its accuracy depended on parameter adjustments made using the trial-and-error method.~~

~~The machine learning model-building process was divided into two main steps: the first was the XGB model building, and the second was the hybrid model building (the integration of XGB with optimization algorithms). The accuracy of the machine learning model depends on the parameter adjustments of the XGB model. In this study, the XGB model parameters were selected using the trial-and-error method. Finally, the XGB parameters were $n_estimators=100$, $max_depth=4$, $subsample=0.5$, and $colsample_bytree=0.5$. While the hybrid model was built by integrating the XGB model and optimization algorithms, namely GOA, POA, SOA, STO, and PSO. To integrate the XGB model with optimization algorithms, we first need to construct an objective function $F(\theta)$ that returns the error value of XGB on the validation set when using the parameter sets θ . That is, each parameter set has a different error value. Next, determine the search space of the hyperparameters ($n_estimators$, max_depth , $subsample$, $colsample_bytree$) as discrete value intervals. Then, the optimization algorithms will initialize the population of~~

individuals with the size and parameters characteristic of each optimization algorithm. This study was tested with 500 iterations: at each iteration, each individual will generate a combination of θ_i , and the optimization algorithms will update the position or velocity of the individuals according to their own rules. This process is repeated until a stopping threshold is set. Finally, the results are the optimal parameters. The parameters of the model are as follows: problem_size = 3, batch_size = 25, epoch = 500, pop_size = 50, "fit_func": fun_avr2, "lb": [0] problem_size, "ub": [1] problem_size, c_min = 0.00004, c_max = 2.0 for **XGB-GOA**; problem_size = 3, batch_size = 25, epoch = 500, pop_size = 50, "fit_func": fun_avr2, "lb": [0] problem_size, "ub": [1] problem_size, c1=2.05, c2=2.05, w_min=0.4 for **XGB-PSO**; problem_size = 3, batch_size = 25, epoch = 500, pop_size = 50, "fit_func": fun_avr2, "lb": [0] problem_size, "ub": [1] problem_size for **XGB-POA**; problem_size = 3, batch_size = 25, epoch = 500, pop_size = 50, "fit_func": fun_avr2, "lb": [0] problem_size, "ub": [1] problem_size for **XGB-SOA**; problem_size = 3, batch_size = 25, epoch = 500, pop_size = 50, "fit_func": fun_avr2, "lb": [0] problem_size, "ub": [1] problem_size for **XGB-STO**.

Formatted: Vietnamese

Evaluation of model accuracy

The statistical indices, the root mean square error (RMSE), the mean absolute error (MAE), and the correlation coefficient (r) were used to assess the accuracy of the proposed models.

Analysis of spatial distribution and identifying the farmers adaptive capacity interview area identification

Formatted: English (United States)

We validated the models and then used them to assess soil salinity in the study area at a pixel scale with a resolution of 10x10 m. After validating the models, they were utilized to assess soil salinity in the study area at a pixel scale with a resolution of 10x10 m. Approximately 30 million pixels were assessed, and a soil salinity map was constructed using the Point to Raster tool in ArcGIS 10.8.

We used the second strand of our methodology, interviews with populations, to evaluate the adaptive capacity of farms in the study area. The second strand of our methodology, interviews with populations, was used to assess the adaptive capacity of farms in the study area. A-Tân We selected An Tan commune in the Thai Thuy district to participate in structured interviews was selected for this assessment. A total of 87 households were interviewed. These households were randomly selected from An Tan commune in the Thai Thuy district to participate in structured interviews. The commune is located in the coastal region, which has the lowest altitude and is often

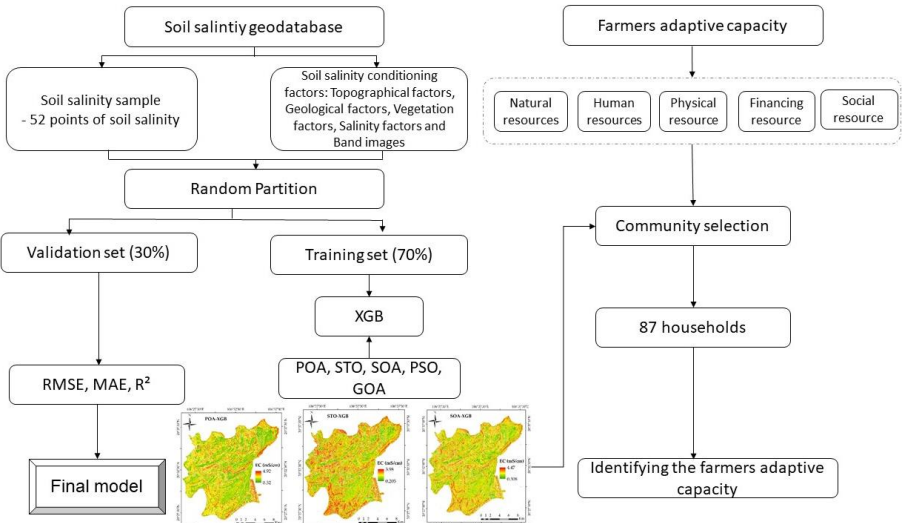
affected by soil salinity. Residents mainly worked in rice and fish farming. We analyzed all 87 responses to assess farmers' ability to adapt to soil salinity. Residents mainly worked in rice and fish farming. All 87 responses were used to analyze farmers' adaptive capacity to soil salinity.

The structured interviews focused on five main elements: natural resources, human resources, physical resources, financial resources, and social resources. There was a particular focus on soil salinity in 2023, allows to evaluate the stress of environment on the livelihood of population 2023.

Formatted: English (United States)

Formatted: English (United States)

Formatted: English (United States)



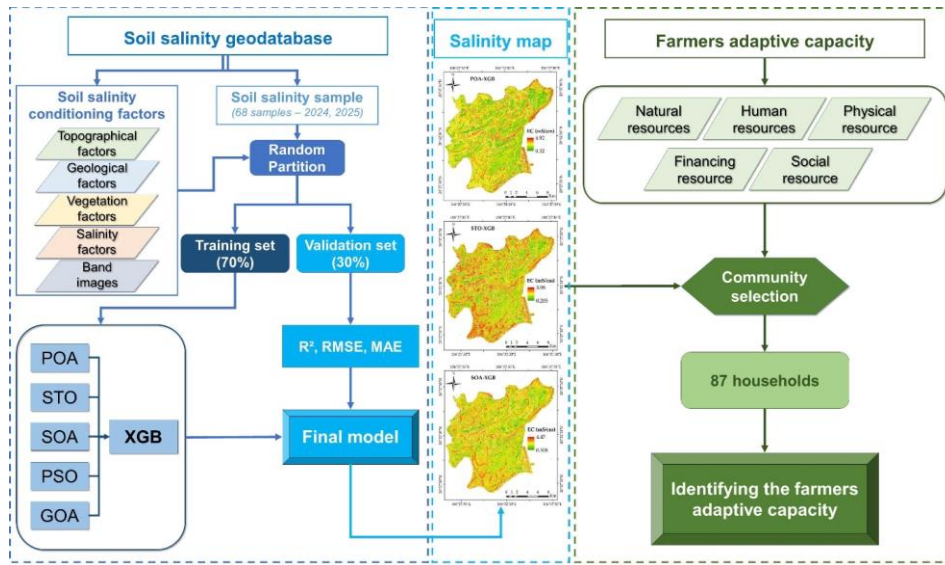


Figure 2: Methodology used for the farmer's adaptive capacity and soil salinity in this study: The methodology used in this study is to design a theoretical framework to assess soil salinity and farmers' adaptive capacity based on machine learning, optimization algorithms, remote sensing, and interviews with local people. We divided this process into four main steps: i) data preparation; ii) machine learning model construction; iii) machine learning model evaluation; and iv) analysis of spatial distribution and identifying the farmers' adaptive capacity.

3.1. XGBoost (XGB)

XGB is a popular gradient-boosted tree algorithm that can solve classification and regression problems. The main idea of learning with XGBoost is to train several models sequentially and combine them successively by correcting errors iteration after iteration to obtain the most potent ensemble model possible (Zhang et al., 2022). Therefore, the prediction result of the prediction is, therefore, consists of a set of chained decision trees made up of the prediction of the set of chained decision trees. This method increases the performance and stability of the model while minimizing its variance (Zhang et al., 2022). The XGB model functions in three main steps: i) it constructs an individual model (tree) by taking predictions on the training data, ii) it computes the mistakes of these predictions for the real values, and iii) it constructs another tree to predict and correct these mistakes. The process is repeated, and each new tree is built to correct the mistakes of the previous one. This phase is called "boosting". We then sum

Formatted: English (United States)

Formatted: English (United States)

Formatted: English (United States)

331 ~~up the predictions of all trees to determine the final predictions~~The predictions of all trees are then summed to take
332 ~~the final predictions~~ (Mukhamediev et al., 2023).

333 To optimize the accuracy of the XGB model, three main parameters need to be adjusted: learning rate (reducing the
334 value of this parameter can avoid the overfitting problem), alpha, and lambda (increasing the value of these
335 parameters makes the model more conservative), and column sample by tree (adjusting this parameter has the
336 objective of obtaining the subsample of columns) (Tan et al., 2023).

337 3.2. Pelican Optimization Algorithm (POA)

338 Agents searching for prey in nature have a mechanism similar to that of agents searching for optimal solutions.
339 Therefore, based on this perspective, the search agents that comprise a population seek to achieve the optimal
340 solution more quickly. Each agent is an optimal solution whose position is determined in the search space. From a
341 mathematical perspective, agents are vectors, and the population of agents forms matrices (Dehghani and Trojovský,
342 2022). Among the values used to calculate the aim function, the top value of the agents is determined as the top
343 solution of the agents.

344 One such optimization algorithm is POA proposed by (Trojovský and Dehghani, 2022). This algorithm is designed
345 based on Pelicans' foraging and communication processes. This is a large bird with a long beak and a large pouch in
346 the throat to hold prey during hunting. Hundreds of individuals may flock together. They can weigh up to 15 kg,
347 grow to a height of 1.8 m, and have a wingspan of up to 3 m. These characteristics greatly assist them in finding
348 food, such as fish, frogs, and turtles.

349 POA is based on the simulation of the ~~ecomportment behavior~~ and plan of pelicans when attacking prey. Pelican
350 hunting strategies are divided into two stages. First, the bird moves towards its prey, then it spreads its wings and
351 glides along the water surface to attack. In the first stage, the pelicans determine the situation of the prey and move
352 toward the identified prey area. Identifying prey areas represents the determination of the search space in the POA
353 model. The positions of the prey are randomly produced in the search space, which increases the exploration power
354 of POA in the process of searching and solving optimization problems. After locating the prey area in the second
355 stage, pelicans spread their wings and move on the water surface to attack the prey and store it in their throat pouch.

Formatted: English (United States)

356 This strategy allows them to capture more prey. Modelling this behavior of pelicans makes the POA model easier to
357 converge and improves local search ability (Alamir et al., 2023; Trojovský and Dehghani, 2022).

358 3.3. Serval Optimization Algorithm (SOA)

359 SOA is one of the population-based optimization algorithms, and ~~they-it~~ exploit the searching power of agents in a
360 population. This property makes this algorithm powerful in solving optimization problems (Dehghani and
361 Trojovský, 2022). ~~Each iteration of SOA continuously determines and updates the agents' situations~~In SOA, the
362 ~~agents' situation are continuously determined and up-to-date in each iteration.~~ The updating process simulates the
363 behavior of serval cats in the wild, divided into two stages: i) exploration of the search space and ii) local
364 exploitation in the search space (Sindi et al., 2024).

365 Wild cats are some of the most efficient predators, using hearing to identify and attack prey. In the first stage of
366 SOA, the situation of the servals is repeatedly up-to-date after each move: the continuous updating of positions
367 guides-leads to detailed coverage of the search space. The ~~aim-of~~ this stage aims is to raise the power to search and
368 explore in the search space. The situation of the best member in the SOA is considered the situation of the prey and,
369 therefore, the optimal solution (Dehghani and Trojovský, 2022; Sindi et al., 2024).

370 When attacking prey, wild cats jump during the chase to prevent the prey from escaping. These strategies also
371 serve~~In SOA, these strategies are also used~~ to update the position of the SOA population. The simulation of the
372 chase process can cause small changes in agents' positions in the SOA. However, this phase aims to increase the
373 search space mining capability of SOA, which helps to improve the local search capability in the search space
374 (Dehghani and Trojovský, 2022).

375 3.4. Siberian Tiger Optimization (STO)

376 The STO algorithm is a new biologically inspired hyper-heuristic algorithm modeled after Siberian tigers' hunting
377 behavior (Trojovský et al., 2022). STO replicates the Siberian tiger tracking and capture strategy, using a
378 population-based approach to explore the search space efficiently and quickly (Trojovský et al., 2022).

379 STO works by simulating the way Siberian tigers move and communicate with each other while hunting their prey.
380 Each agent in the STO algorithm represents a Siberian tiger, ~~each~~-exploring a different region in the search space.
381 The tigers communicate and share information about their locations with each other to find the optimal location. The

Formatted: English (United States)

location update process of Siberian tigers in STO is carried out in two main phases: the hunting and bear-fighting phases (Trojovský et al., 2022).

In the hunting phase, since the Siberian tiger is a powerful predator, it hunts by ~~attacking~~ ~~assaulting~~ different prey, so the agents in the STO are up-to-date based on the simulation of this hunting strategy. After choosing the prey, the Siberian tiger will chase, attack, and kill its prey in this phase. The population continuously updates the members' positions based on the selection and attack of the prey.~~The members' positions of the population are continuously updated on the choice and attack of the prey.~~ This phase causes sudden changes in the members' positions and increases the search ability in the search space (Al-Sarray et al., 2024).

During hunting, the Siberian tiger has to fight with brown and black bears. Therefore, in the second phase, the members of the STO ~~are up-to-date~~ ~~stay update~~ on the ~~policy~~ ~~strategies used by the~~ of the Siberian tiger when ~~fighting with bears~~ ~~bear-fighting~~. When fighting with bears, the Siberian tiger ambushes and then assaults the bear until it kills it (Al-Sarray et al., 2024; Trojovský et al., 2022).

One of the key features of STO is its ability to balance exploration and exploitation. In ~~other words~~ ~~put it another~~ way, the design of the STO algorithm is designed to explore~~explores~~ involves extensive exploration of the search space ~~extensively~~ and ~~refine~~ ~~refinement of~~ promising solutions in the most promising areas. Thus, STO avoids local optimization problems and increases the likelihood of global optimization (Trojovský et al., 2022).

3.5. Particle Swarm Optimization (PSO)

PSO was proposed by (Kennedy and Eberhart, 1995). It is founded on the principles of self-organization that allow one or more groups of living organisms to move together in a complex way (Fu et al., 2018). PSO simulates the movement process of some animals, such as flocks of birds. In this model, birds move randomly by following three rules: i) they track the same path as their friends, ii) they are enticed to the average situation of the group, and iii) they maintain a certain space between each other to avoid collisions (Ruidas et al., 2022).

PSO explores the search space through the birds' position and flight paths. The position of each bird in the search space is considered a potential solution. More precisely, the position and speed of the birds are represented by vectors with D dimensions, and the initial speed is determined randomly. In the PSO algorithm, the position and velocity of each bird are updated continuously after each iteration until an optimal solution is reached. The

Formatted: English (United States)

Formatted: English (United States)

Formatted: English (United States)

Formatted: English (United States)

Formatted: English (United States)

Formatted: English (United States)

optimization function ~~assesses the position and velocity quality is used to evaluate the quality of the position and velocity~~(Bui et al., 2016). In this study, PSO was used to optimize the XGB model.

3.6. Grasshopper Optimization Algorithm (GOA)

GOA was first proposed by (Mirjalili et al., 2018). This algorithm is based on the swarm behavior of locusts during foraging to solve optimization problems. Grasshoppers move quickly to explore spaces, and then they move locally to exploit resources in the foraging space. GOA models the behavior of a virtual swarm of grasshoppers, where each position represents an optimization solution to the problem (Moayedi et al., 2021; Nguyen, 2022). Movement is influenced by several factors: social interaction, gravity, and wind advection. Social interaction plays an important role in finding the optimal position because grasshoppers interact with each other to exchange information about precise positions. This social communication allows grasshoppers to find the right solutions. Then, gravity allows grasshoppers to explore the foraging spaces in a balanced manner, hence avoiding the local optimization problem (Ingle and Jatoth, 2024). Finally, wind advection represents the external effects that can influence the movement of grasshoppers, leading them to some areas of the search space. In the optimization process, an equilibrium between exploration and exploitation is important to accurately approach the true global optimum (Moayedi et al., 2020).

4. Results

4.1. Soil Salinity Predictors

The choice of suitable factors plays a key role when using machine learning to determine the geographical distribution of soil salinity in any region. Conditioning factors represent the causes of soil salinity, so improper selection of these factors can result in inaccurate prediction. Data redundancy may complicate the model and lead to poor performance~~Data redundancy may make the model more complex and lead to poor performance.~~

In this study, we used RF to measure the appropriate factors~~RF was utilized to measure the suitable factors in this study.~~ It assigns a value to each factor based on ~~the relation~~its relationship with the soil salinity~~within soil salinity~~ samples and the conditioning factors. The most important factor is the one with the greatest importance in determining soil salinity zones. In addition, after using RF to determine the importance of factors, we used trial and error to continue eliminating factors that affected the precision of the model.

433 The outcome showed that six factors (DEM, RVI, B2, S6, S2, and S1) had an RF value of zero, so these factors did
434 not affect the determination of the spatial distribution of saline areas. In addition, two factors (NDVI and flow
435 accumulation) were eliminated using the trial-and-error method. The other 30 factors were used to build the model.
436 VVVH (0.39), VV (0.3), distance from the river (0.28), CRSI (0.24), and EVI (0.21) had a strong influence on the
437 soil salinity in the study area. S3 (0.17), BI (0.17), B12 (0.15), SI2 (0.14), B7 (0.11), VH (0.1), and Int2 (0.1) have
438 moderate relationships with the soil salinity. B11 (0.08), S5 (0.06), slope (0.06), SI (0.06), SAVI (0.06), NDSI
439 (0.06), SI4 0.05), B5 (0.05), Int1 (0.05), B9 (0.05), B4 (0.05), SI (0.04), SI1 (0.04), B8 (0.04), B3 (0.02), B1 (0.02),
440 and B6 (0.02) had only a weak relationship on soil salinity (Figure 3).

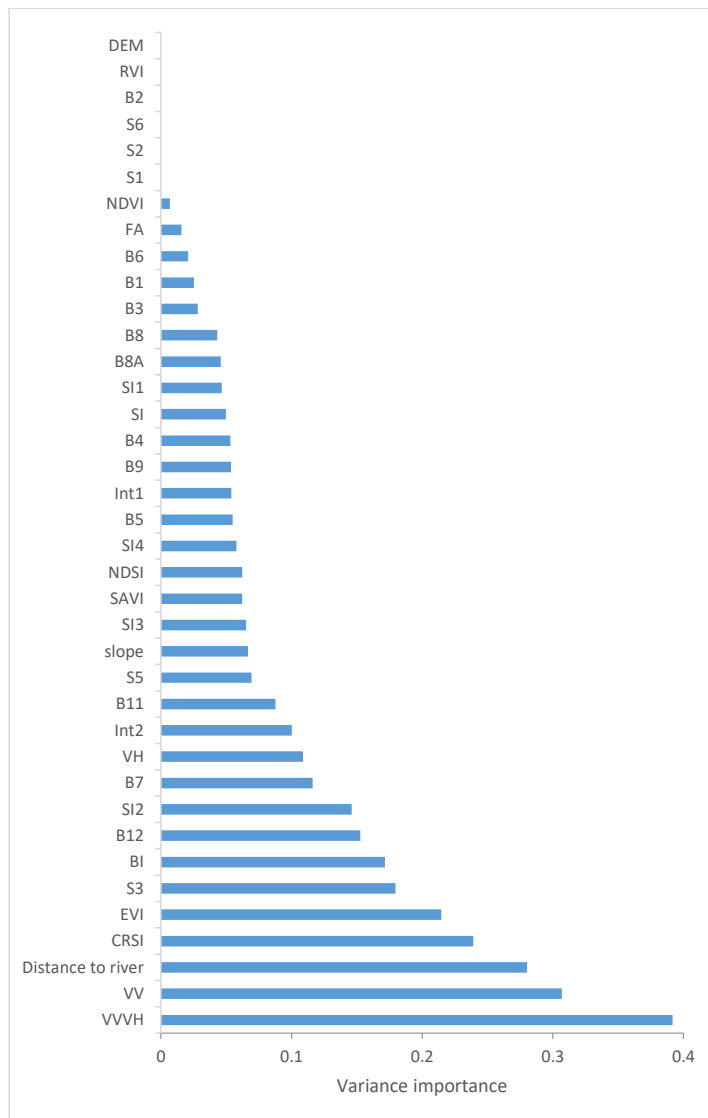
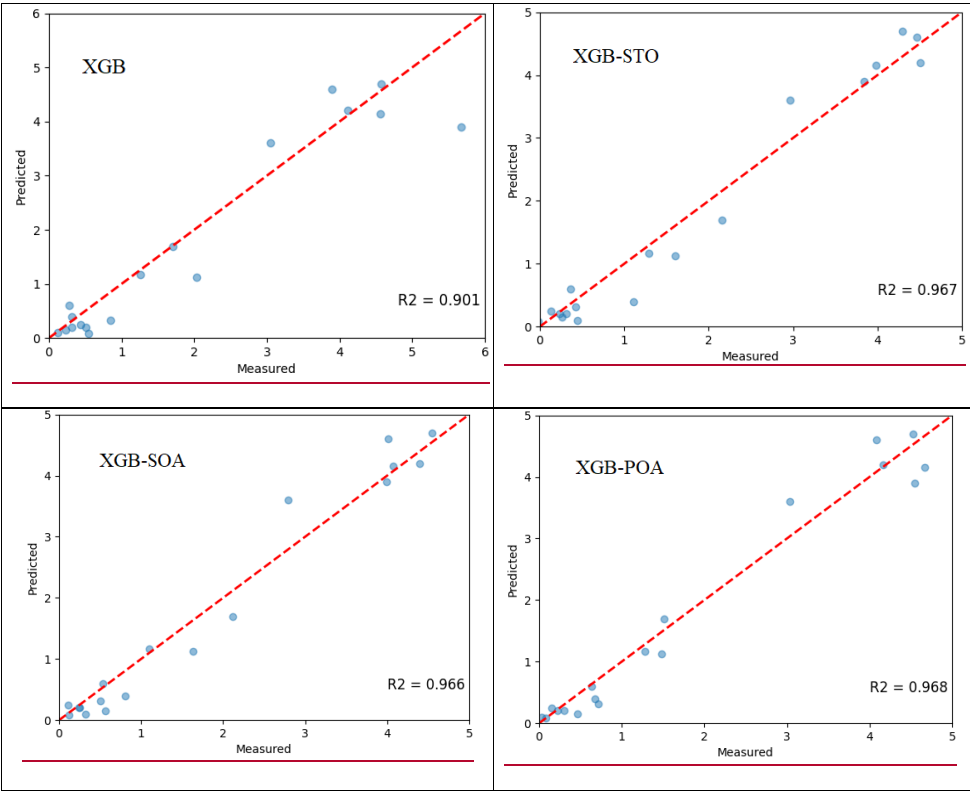


Figure 3: Variables important for soil salinity model using RF.

445 **4.2. Model Accuracy Validation**

446 R^2 was used to assess the performance of the machine learning models. The outcome of this study demonstrated that
447 all optimization algorithms enhanced the performance of the XGB model. The XGB-POA model was the greatest,
448 with an R^2 value of 0.968, followed by XGB-STO ($R^2=0.967$), XGB-SOA ($R^2=0.966$), XGB-PSO ($R^2 = 0.964$), and
449 XGB-GOA ($R^2=0.964$; Figure 4).



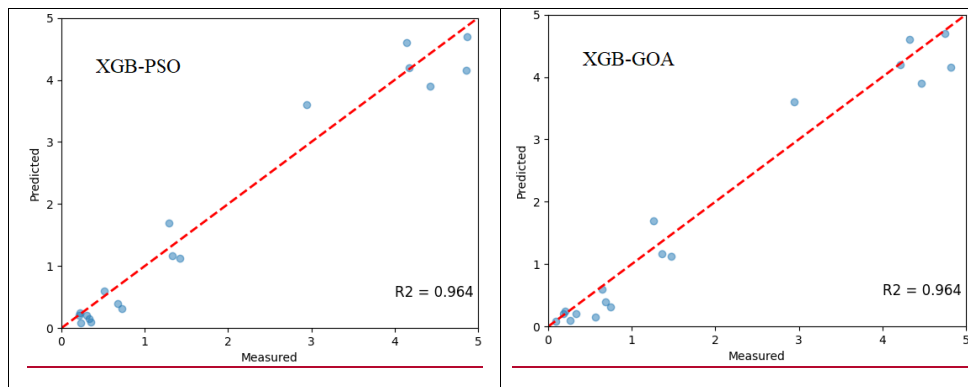


Figure 4: R^2 value for the testing dataset

The RMSE and MAE were also used to evaluate the accuracy of the machine learning models. The XGB-POA model performed better on training and validation data (RMSE=0.28, MAE=0.18 for learning data and RMSE=0.31 and MAE=0.242 for verification data). The XGB-STO was ranked second with an RMSE value of 0.3 and MAE of 0.22 for learning data, and an RMSE value of 0.32 and MAE of 0.244 for verification data. The XGB-SOA model was ranked third, with RMSE=0.31 and MAE=0.23 for learning data and RMSE=0.33 and MAE=0.25 for verification data. XGB-GOA model came fourth, with RMSE=0.33 and MAE=0.25 for learning data and RMSE=0.34 and MAE=0.26 for verification data. The XGB-PSO model performed less well than the other models, with RMSE=0.335 and MAE=0.26 for learning data and RMSE=0.341 and MAE=0.27 for verification data (Table 1).

Table 1. Model performance and comparison.

Models	Training dataset			Validation dataset		
	RMSE	MAE	R^2	RMSE	MAE	R^2
XGB-POA	0.28	0.18	0.99	0.31	0.242	0.968
XGB-STO	0.3	0.22	0.987	0.32	0.244	0.967
XGB-SOA	0.31	0.23	0.98	0.33	0.25	0.965966
XGB-GOA	0.33	0.25	0.97	0.34	0.26	0.964
XGB-PSO	0.335	0.26	0.97	0.341	0.27	0.964

XGB	0.35	0.32	0.91	0.37	0.34	0.901
------------	------	------	------	------	------	-------

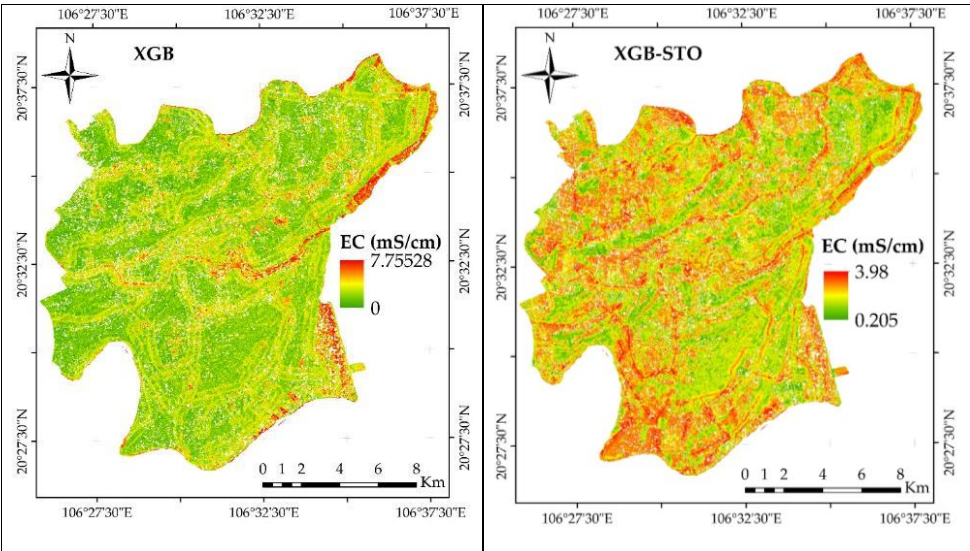
4.3. Spatial distribution of soil salinity in the Thai Thuy district of the Red River Delta

Following validation, we constructed a geographical distribution map of soil salinity using the proposed models. We carried out the process by assigning conditioning factors to the 30 million pixels across the entire study area. Depending on each model, the EC value varies from 0.29 to 7.7 mS/cm. On the map, the color varies from green to red, representing different EC values. The areas with green colors are located far from the continent (EC = 0.29), while the areas with red colors are located on the coast, with EC values superior to 7.7 mS/cm. This graph shows that these areas are directly affected by saltwater intrusion from the sea (Figure 5).

According to the FAO, salinity can be divided into 5 levels: non-saline, slightly saline, moderately saline, heavily saline, and very heavily saline. In which the EC value is below 2 mS/cm, the soil is considered not saline, and the plants grow completely normally. The EC value ranges from 2- 4 mS/cm; the soil is slightly saline and has very little effect on the plants. Specifically, flower crops may grow slowly, while rice and fruit trees may have reduced height. The EC value ranges from 4-8 mS/cm; the soil is moderately saline and reduces crop yields. Specifically, rice can have a 10-20% reduction in yield. The EC value ranges from 8 - 16 mS/cm; the soil is heavily saline and affects the growth of plants. The soil becomes extremely saline and uncultivated if the EC value surpasses the threshold of 16 mS/cm. This study utilizes the XGB-POA model, which boasts the highest accuracy, to analyze the areas affected by saline intrusion. Specifically, in the study area, about 65 km² of land area is not affected by saline intrusion, 165 km² is slightly affected, and 1.8 km² is greatly affected by saline intrusion. Compared to the land cover/land use map, it can be seen that the land area greatly affected by saline intrusion is mainly aquaculture; therefore, this area will not be significantly affected in terms of productivity. Meanwhile, 165 km² of land affected by saline intrusion is rice land, which can slow down rice growth and reduce productivity.

In the study area of Thai Thuy District, Thai Binh Province, about 70-75% of the agricultural land is irrigated by a canal system that draws water from the Red River and the Day River. Thanks to the water source from the Red River and the Day River, agricultural production areas are regularly washed away with salt, so the EC value in these areas is often below 4 mS/cm. In coastal areas, salinity intrusion at river mouths forces people to use shallow groundwater for irrigation, which leads to salt accumulation and prompts a shift from rice cultivation to

487 aquaculture. After validation, the proposed models were used to construct a geographical distribution map of soil
 488 salinity. The process was done by assigning conditioning factors to the 30-million pixels for the entire study area. It
 489 can be seen that the EC value varies from 0.29 to 7.7 mS/cm, depending on each model. On the map, the color varies
 490 from green to red, representing different EC values. The areas with green color are located far from the continent
 491 (EC=0.29), while the areas with red color are located on the coast, with EC value superior 7.7 mS/cm. This shows
 492 that these areas are directly affected by saltwater intrusion from the sea (Figure 5).



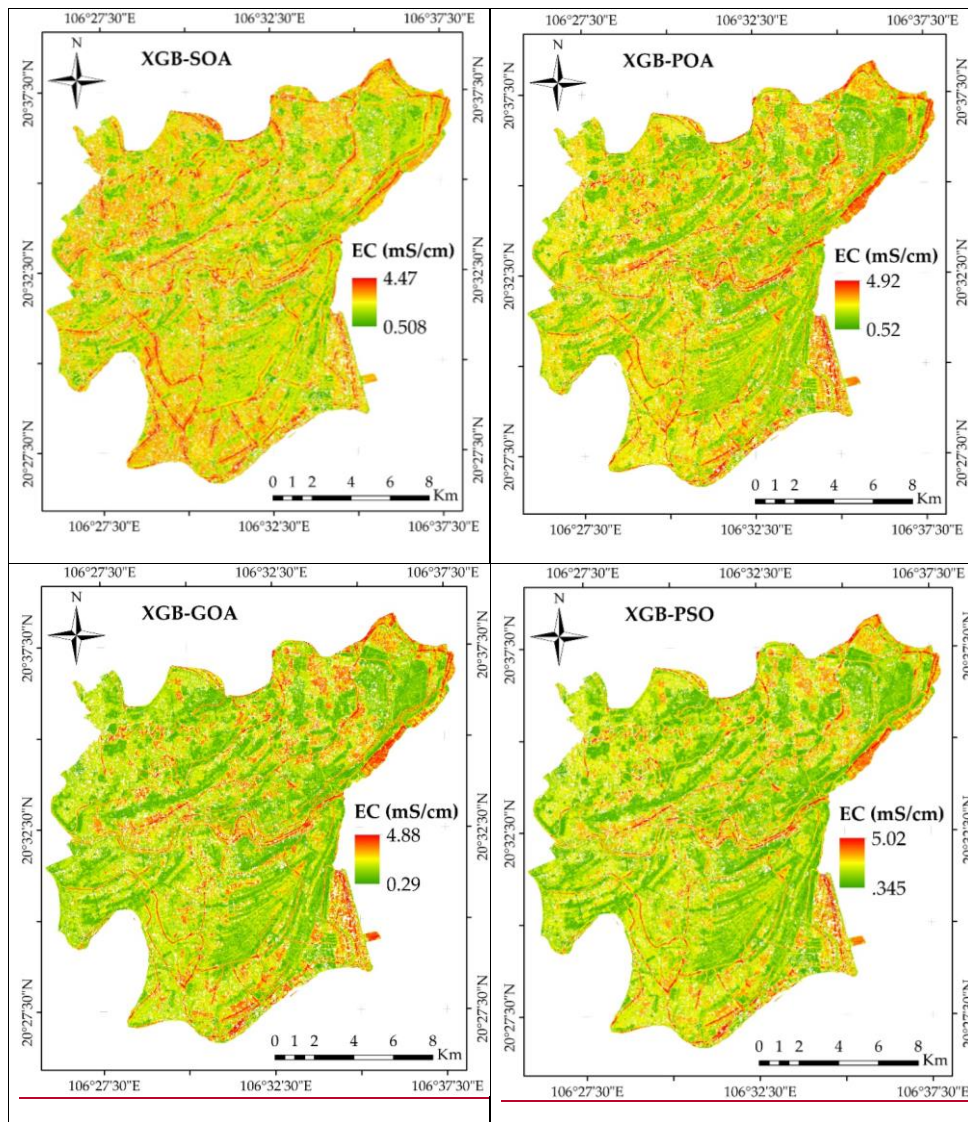


Figure 5: Soil salinity mapping in the Thai Thuy district

4.4. Farmers' Adaptive Capacity Assessment

Soil salinity is a key challenge for deltas worldwide, particularly in deltas where population density is high and socio-economic conditions are poor (Hoque et al., 2016). The Red River Delta is the most densely populated area in Vietnam and one of the most densely populated deltas in Southeast Asia; therefore ~~it is crucial~~~~it is key~~ to consider the impact of soil salinity in this delta on the farmer's life and their adaptive capacity. Spatial distribution maps of soil salinity show that this phenomenon occurs in many areas of the Thai Thuy district, especially in coastal areas.

~~This phenomenon certainly has a significant impact on people's living conditions and production areas, posing challenges to their livelihoods. In this section, we address the adaptive capacity of farmers in An Tan commune, a coastal area, through five elements: i) natural resources including land use, awareness of saline intrusion, perceived impacts on agricultural activities, and adaptation measures taken, ii) human resources such as household demographics, education, and farming experience, iii) physical resources, including the availability of farming equipment and infrastructure, iv) financial resources focusing on household income, income structure, credit access, and changes over time, and v) social resources addressing support from government and social networks, community cooperation, and participation in collective adaptation activities. We interviewed 87 households in the An Tan commune to analyze the community's ability to adapt to saline intrusion. This certainly significantly impacts people's living and production areas and poses challenges to their livelihoods. In this section, we address the adaptive capacity of farmers in A Tan commune, a coastal area, through five elements: natural resources, human resources, physical resources, financial resources, and social resources. To analyze the community's ability to adapt to saline intrusion, 87 households in the A Tan commune were interviewed.~~

4.4.1. Natural Resources

Due to the process of ~~salinity~~~~salinization~~, we are facing a major threat to agriculture and sustaining arable land. Excess salinity adversely influences soil structure and fertility, plant growth, crop yield, and microorganisms (Tarolli et al., 2024). Soil salinity is frequently associated with water salinity. Groundwater in littoral regions of the Red River Delta is characterized by high salinity (Hoque et al., 2016). The scarcity of freshwater poses significant challenges for crop irrigation. Irrigating with saline water exacerbates soil salinity. In addition, soil salinity also creates a scarcity of grazing land and fodder cropland of coastal areas. Coastal livestock is harshly suffering from food inaccessibility and poultry farming in the coastal districts. All the mentioned factors impose considerable risks

to the coastal inhabitant's livelihood and food security, who rely mainly on agricultural activities such as growing rice and crops such as onions, garlic, watermelon, and tobacco, according to our interviews.

Indeed, the results showed that 59% of interviewed households said that salinization ~~had~~ had a medium to high impact on agricultural production in the area in recent years, especially during the 2023 saline intrusion. Meanwhile, 38% of households stated that saline intrusion has little or very little impact on agricultural production, mainly households in areas far from the coast and so less affected. Households in the study area have ~~taken-implemented~~ ~~many-various~~ measures to mitigate the increasingly serious saline intrusion, such as washing the salt ~~from the fields~~ after each crop (as instructed by local authorities) and ~~changing the crop structure~~ ~~adjusting their cropping systems~~ ~~by adopting salt-tolerant crop varieties or transitioning to aquaculture practices~~. 66% of interviewed households said they had to change the crop structure to suit the saline intrusion or switch to non-agricultural occupations to earn more income. Of the 87 households interviewed, 28% had their main income from non-agricultural activities. A large number of people switching to non-agricultural activities can meet their livelihood needs, but in the long-term, farmers abandoning agricultural activities to seek jobs in factories or migrate to cities also poses many negative environmental and social consequences, such as the decline of agrobiodiversity or labor shortages in agriculture, etc. (Subedi et al., 2022).

4.4.2. Human Resources

In agricultural production and the adaptability of the community to salinity intrusion, demographics are considered one of the most important factors contributing to the creation of labour resources, directly affecting crop productivity. The results of interviews with 87 households showed that each household has an average of 3.5 members, comprising 2.5 workers and 1 dependent member. Using available family resources reduces labor costs, thereby increasing production profits. However, the quality of human resources poses a concern when adapting to saline intrusion. One of the criteria for evaluation is education level. Most workers in households had a junior high school degree (66%), 5% of interviewees had a high school degree, and less than 3% had a university degree. According to previous studies, education is an important factor in determining workers' income. In the context of climate change and sea level rise, agriculture is negatively affected by these phenomena: low levels of education mean a lesser ability to absorb new knowledge and methods in organizing production to reduce the negative impacts of saline intrusion. Although 83% of the interviewed households had more than 20 years of experience in

548 agricultural production, their knowledge of saline intrusion and climate change was still limited. Specifically, people
549 lack the adequate knowledge and skills to adapt to changes in environmental conditions, leading to difficulties in
550 choosing appropriate livelihood models.

551 Furthermore, saline intrusion has led to several health insecurity. Coastal residents in saline areas are at risk of
552 consuming high salt above the recommended levels. It is evaluated that over 7 million coastal populations in
553 Bangladesh, India, and Vietnam suffer from hypertension and cardiovascular diseases as a result of long-term
554 ingestion of saline groundwater (Hoque et al., 2016). This has profound consequences for the development and
555 quality of human resources in these areas.

556 4.4.3. *Physical Resources*

557 Material resources include essential items that serve people's daily life and livelihoods. The majority of the
558 households interviewed were engaged in agriculture, so the means of production were mainly related to agricultural
559 activities. Of the 87 households interviewed, 90% were equipped with agricultural production equipment such as
560 pumps, sprayers, and tractors, while 100% had access to tractors and harvesters for farming. The interviewed
561 households used equipment to exploit water sources for agricultural production; however, because the town of An
562 Tan is located in a coastal area, groundwater and surface water are often affected by saline intrusion. Thus, they still
563 faced challenges related to water resources, especially in the context of saline intrusion

564 Moreover, in response to saline intrusion, accessing freshwater for daily use and irrigation often leads to the
565 spontaneous extraction of groundwater through tubewells, a common practice in coastal areas of Vietnam and
566 Southeast Asia (Hoque et al., 2016). However, excessive groundwater extraction and improper irrigation practices
567 also pose many potential risks of increasing water resource depletion and accelerating salinization processes (Tarolli
568 et al., 2024). This will likely undermine the long-term adaptive capacity of coastal communities.

569 4.4.4. *Financial Resources*

570 The interviews with 87 households demonstrated that 9% of the households interviewed were poor and near-poor. It
571 can be seen that economic status greatly affects people's ability to adapt and recover from soil salinity. Poor and
572 near-poor households frequently have more difficulty evaluating solutions to mitigate the impact of soil salinity on
573 agricultural production. The primary source of income for a large part of the population mainly comes from

574 agricultural activities: 72% of the households interviewed confirmed that their main livelihood was agriculture.
575 However, their agricultural income is frequently unstable. This stresses the vulnerability of people's livelihoods due
576 to the strong effects of soil salinity on agricultural activities. Meanwhile, 56% had a stable source of income from
577 factory work. This emphasizes the need to diversify income sources for inhabitants in soil salinity areas. In addition,
578 although the income from agricultural production was enough to cover farmers' daily life, most of the households
579 interviewed could not save. Therefore, with increasing saline intrusion in the context of climate change, it is very
580 difficult for these households to have an effective response or adaptation solutions. Borrowing capital to overcome
581 the negative impacts of saline intrusion is one of the adaptation strategies reported by the interviewed households.
582 36% of households borrowed capital from relatives, 11% borrowed from credit funds or banks, 14% from local
583 organisations, and 33% from distribution agents. Meanwhile, 8% of the interviewed households could not borrow
584 any capital to overcome the consequences of saline intrusion.

585 Diversifying external sources of capital can help households overcome the consequences of saline intrusion and
586 support agricultural production more generally. However, there are still several people who cannot access capital
587 sources, and training to the adaptability and resilience of the people. This increases the impact of soil salinity on the
588 community in the study area. Furthermore, a capital utilization strategy must be carefully considered to ensure
589 efficient use of resources to improve livelihoods and enhance adaptability to saline intrusion.

590 4.4.5. *Social Resources*

591 Social resources play a key role in mitigating the impacts of soil salinity on the adaptability and resilience of the
592 people. In the study area, households received support from various sources, such as local communities, volunteer
593 organizations, non-governmental organizations, and mutual assistance among households. This support includes
594 exemption from land use tax, support for production equipment, crops, and food supply for people. Regarding
595 people's awareness of climate change and its impact on salinity intrusion, about 82% of households said they learned
596 about this issue through local authorities and media propaganda.. Furthermore, 100% of the households surveyed
597 reported that local authorities also had organised training sessions and drills to respond to saline intrusion and sea
598 level rise. However, as mentioned above, the knowledge and skills of inhabitants are still limited. This raises
599 questions about the effectiveness of training sessions. In addition, these training activities occur infrequently. For

600 example, during the 2soil salinity, people did not receive timely support and assistance from these organisations.
601 This led to a reduction in the community's ability to adapt 4soil salinity.

602 5. Discussion

603 Soil salinity is a global environmental threat, a key cause of food insecurity worldwide (Song et al., 2024).
604 Therefore, it is essential to monitor it with high precision, as is identifying the adaptive capacity of those in
605 vulnerable regions.

606 In Vietnam, two large deltas ensure food security not only, but also in other countries. Although several previous
607 studies have been conducted to assess soil salinity in Vietnam, most have focused on assessing soil salinity and
608 farmers' adaptive capacity in the Mekong Delta (Hoang and Hai, 2024; Nguyen et al., 2024). Research on the Red
609 River Delta is scarceFew studies have been conducted in the Red River Delta. The Red River Delta is one of the key
610 agricultural regions in Southeast Asia. Therefore, assessing soil salinity and farms' adaptive capacity in this area is
611 necessary. In this study, remote sensing, machine learning, and community interviews were used to evaluate soil
612 salinity and the adaptive capacity of farms in the delta.

613 Remote sensing plays a key role in analyzing soil salinity because the salt in the soil has a significant effect on the
614 spectral reflectance of the soil. Soils with different salinity levels will have different spectral characteristics; for
615 example, areas covered with white salt often have higher spectral reflectance levels and salinity (Hoa et al., 2019;
616 Wu et al., 2018; Xiao et al., 2023). This is the basis for using remote sensors to monitor saltwater intrusion.
617 However, one of the challenges in using Sentinel 2 satellite images in soil salinity monitoring is that sometimes , the
618 spectral reflectance level is not consistent with soil salinity. Many studies have integrated vegetation indices in soil
619 salinity monitoring to minimize this limitation because different areas will have different soil salinity. It should also
620 be noted that the difference depends on the vegetation type in each area. Therefore, this study has integrated Sentinel
621 1 images in soil salinity monitoring. Sentinel 1 images use radar signals to monitor moisture and dielectric
622 properties providing accurate information on soil salinity. This is particularly important in coastal areas, where
623 surface moisture is high, reducing the accuracy of optical imagery. This approach identifies areas severely affected
624 by salinity intrusion while supporting the assessment of the adaptive capacity of communities in the area (Hoa et al.,
625 2019). However, with the increase in the volume, type, and speed of remote sensing data collection, bottlenecks in

the data analysis process may occur (due to the inadequacy of the structure of current models for processing large datasets).

XGB is one of the most powerful algorithms for identifying the spatial distribution of natural hazards, such as floods, landslides, and soil salinity. Its advantages include the ability to avoid the overfitting problem and fast convergence. Additionally, XGB effectively handles missing values (Liu et al., 2022; Mo et al., 2019). However, both the configuration and interpretation of XGB are more complex, and the parameters of this model are also complex to tune. Incorrect parameter selection can reduce performance (Ramraj et al., 2016). Therefore, it is necessary to use optimization algorithms to select the parameters of this model. In this study, five optimization algorithms, namely POA, STO, SOA, PSO, and GOA, were utilized to optimize the parameters of XGB. The XGB-POA model outperformed the other models as it is easy to carry out, has few parameters to adjust, has faster convergence capability, and can avoid local minima - which enables it to find the best global solution (Premkumar and Santhosh, 2024). Previous studies have indicated that POA also can solve complex problems with a large number of variables and non-linear properties (Alamir et al., 2023; Li et al., 2023). XGB-STO model ranked second. The STO algorithm maintains a good equilibrium with exploration and exploitation processes. This allows it to avoid local minima problems, which improves model performance (Al-Sarray et al., 2024; Trojovský et al., 2022). The XGB-SOA model came third in terms of accuracy. SOA can solve complex problems with a large number of variables or continuous, discrete, or multi-objective problems, so it is a versatile tool for several different applications. In addition, inspired by the serval's precise jumps and fast movements, SOA can converge quickly with high accuracy (Dehghani and Trojovský, 2022; Sindi et al., 2024). The XGB-PSO model was ranked fourth. In addition to ease of use, PSO has the advantage of equilibrium of the exploration and exploitation processes. This can avoid the local optimization problem (Juneja and Nagar, 2016; Rini et al., 2011). The XGB-GOA model was less accurate than other models because it tends to concentrate exploration at the beginning of the process to avoid the local optimization problem. This may lead to slow convergence (Mirjalili et al., 2018; Zhao et al., 2019). When comparing the models proposed in this study on the ability to predict natural hazards such as soil salinity, each model has different characteristics that influence the real-time prediction ability. Three models (XGB-POA, XGB-STO, and XGB-SOA) can converge quickly because of the faster learning speed. Therefore, these models best suit adaptation for real-time applications because fast updates are necessary to support those tasked with developing mitigation strategies.

654 The results of this study not only confirmed the effectiveness of XGBoost models in soil salinity prediction but also
655 showed the potential for improving accuracy by combining them with optimization algorithms. Compared with
656 previous studies, the models in this study outperform traditional models. (Wang and Sun, (2024) used three machine
657 learning models, namely random forest (RF), support vector machine (SVM), and artificial neural network (ANN),
658 to predict the soil salinity in Huludao City, China. The results indicated that the RF model performed better with an
659 R² value of 0.84. The model accuracy in Wang and Sun's 2024 study was lower than the models in our study.
660 (Aksoy et al., (2024) applied two models, namely XGB and RF to predict the soil salinity in western and
661 southeastern Lake Urmia Playas (LUP) in the Northwest of Iran. The results showed that the XGB model was more
662 efficient with the R² value of 0.83. It was less accurate than in our study. (Elsheawy et al., (2024) evaluated the soil
663 salinity in Sharkia Governorate, Egypt, using four machine learning models, namely support vector machines
664 (SVM), regression trees, Gaussian linear regression, and tree-based ensemble. The results indicated that the SVM
665 model performed better with an R² value of 0.86. Comparison with previous studies showed the potential of the
666 machine learning model in this study to predict soil salinity.

667 Saline intrusion in the Red River Delta and the study area reflects the interaction between natural factors and human
668 activities. One cause of the increasingly serious saline intrusion in the study area is the reduced flow in the delta
669 caused by the construction of dams and reservoirs upstream in China. This reduction reduces the ability of the river
670 system to repel salt water, creating conditions for seawater to penetrate deep into the inland. (Hien et al., (2023)
671 have emphasized that by 2050, saltwater intrusion is likely to extend about 20 km inland from the river mouth,
672 related to sea level rise and reduced discharge from the upper river. (Nguyen et al., (2017) reported that the
673 increasing trend of saline intrusion is the result of sea level rise, combined with the decline of the Red River water
674 level, especially in the dry season. Specifically, the sea level increased by 0.19 m in the period 1901-2010, with an
675 average rate of 3.2 m from 1993-2010. In addition, the phenomenon of saline intrusion is increasingly severe due to
676 subsidence related to groundwater exploitation. In many areas of the Red River Delta in general and the study area
677 in particular, uncontrolled groundwater exploitation for agricultural production and aquaculture contributes to
678 subsidence, increasing the impact of tides. (Nguyen and Takewaka, (2020) have emphasized that the subsidence
679 phenomenon in the delta can reach -12.3 mm/year, which is one of the causes that aggravate the problem of
680 saltwater intrusion, especially in the context of rising sea levels.

Formatted: English (United States)

Field Code Changed

Formatted: English (United States)

Formatted: English (United States)

Field Code Changed

Formatted: English (United States)

Field Code Changed

Formatted: English (United States)

Formatted: English (United States)

Formatted: English (United States)

Formatted: English (United States)

681 The results of this study explored the adaptive capacity of farms in the Thai Thuy district of Thai Binh province.
682 Riverine farmers in areas affected by saltwater intrusion are prepared. They rely on their local communities and
683 expect support from local authorities and voluntary organisations. Our results are similar to those of previous studies
684 investigating the adaptive capacity of residential communities to natural hazards, including saltwater intrusion. The
685 key to adaptation is education, knowledge, and resources to cope with saltwater intrusion. These resources can be
686 natural, physical, financial, social, and human resources.

687 The community's adaptive capacity in the study area faces many challenges, especially in the context of global
688 warming and growing saltwater intrusion. Although most households surveyed have more than 20 years of
689 experience in agricultural production and benefit from available labor resources, their adaptive capacity to saltwater
690 intrusion remains limited. This is in part because these households lack the knowledge to change their livelihood
691 patterns in addressing varying environmental situations. In addition, the main sources of agricultural income are
692 often unstable, and the ability to accumulate finances is low, leading to difficulties in adapting to and recovering
693 from saltwater intrusion. People's adaptation strategies, such as uncontrolled groundwater extraction and conversion
694 to non-agricultural activities, also present long-term environmental and social risks. Furthermore, policies and
695 support programs for residents, such as training sessions and lending programs provided by stakeholders, also raise
696 concerns regarding their effectiveness and inclusiveness. Although people in the study area have access to capital
697 from many different sources, some households still cannot access these sources of capital to overcome the
698 consequences of saltwater intrusion. All of these factors impact agriculture and human life, leading to increased
699 household vulnerability. To enhance people's adaptive capacity, it is important to emphasize the role and
700 effectiveness of policies of local governments, policymakers and stakeholders in supporting people to understand
701 better and respond to saline intrusion. Information and knowledge sharing can be done through direct outreach to
702 people to raise awareness of saline intrusion among communities. Lending policies of local governments and
703 stakeholders need to cover all households while improving the efficiency of capital use. Effective management of
704 natural and physical resources and enhancing social capital through the development of cooperative community
705 models are important factors contributing to people's adaptive capacity to saline intrusion. This study has
706 successfully built a theoretical framework using machine learning with optimization algorithms, remote sensing, and
707 farmer interviews to determine the spatial distribution of soil salinity and farmers' adaptation capacity. However, to
708 apply this theoretical framework in different regions, it is necessary to use factors specifically pertinent to each

709 region. Machine learning models must be provided with the local characteristics of the region in question. However,
710 data collection in any region is difficult, often due to restrictive data-sharing policies or limited financing resources
711 to maintain and distribute the data.

712 From field surveys, it can be seen that in the Red River Delta, adaptation options to soil salinity mainly rely on
713 upgrading the sea dike system, river dikes, and saline prevention sluice systems. In addition, other adaptation
714 options mainly include increasing the resilience of the current agricultural system, such as changing the crop
715 calendar, changing crop varieties, using fertilizers, and planting mangroves. Many households have transitioned
716 from rice cultivation to aquaculture in coastal areas, where soil salinity has a significant impact. In addition, some
717 fish farming households have also switched to shrimp farming or fish farming due to increased saline intrusion.
718 Some households do not have the capital to convert their agricultural systems, and while agricultural productivity
719 decreases due to saline intrusion, they consider finding non-agricultural jobs or migrating to the city to find jobs
720 with more stable incomes. Households located further inland, less affected by saline intrusion, still maintain
721 traditional agriculture. Some households practice intercropping by growing rice alongside vegetables to increase
722 their income. Thus, it can be seen that the adaptability of households in the Red River Delta is not only based on
723 strengthening the system of sea dikes, river dikes, and salinity prevention sluices, but also on transforming the
724 traditional agricultural system to minimize the impact of salinity intrusion. However, capital barriers force many
725 households to abandon agriculture, seriously affecting the food security situation in the region.

Formatted: Vietnamese

726 A significant problem when using machine learning is that of extrapolation. Each model built is adapted only to one
727 set of data. Therefore, evaluating the soil salinity in other regions is challenging. ~~Machine learning models require~~
728 ~~stationarity due to the abrupt and non-stationary nature of the system.~~ General, there is only one model that fits each
729 training dataset. In theory, this would not be a problem if enough training data were collected and all extreme events
730 were included. However, in practice, it is very difficult to collect data for all these events, especially in the context
731 of climate change and sea level rise. To solve this problem, several studies have pointed out that integrating
732 machine learning with conventional models for example, remote sensing or hydrodynamic models can be effective,
733 as such traditional models can provide the training data to use as the input file of the machine learning model.
734 Another solution is to combine machine learning with optimization algorithms, as in this study, to enhance the
735 prediction capability of the machine learning model (Tran and Kim, 2022).

Formatted: English (United States)

736 This study emphasizes the significance of combining machine learning methods to analyze the spatial distribution of
737 salinity intrusion with the community's adaptive capacity to soil salinity. The salinity intrusion map from the
738 machine learning model shows a clear difference in the level of salinity intrusion between coastal, riverside, and
739 inland areas.s. Coastal and estuarine areas often have high levels of salinity intrusion, with EC values exceeding 7
740 mS/cm. These are also areas where communities must apply appropriate adaptation strategies, including crop
741 restructuring, selecting more salinity-tolerant plant varieties, combining agriculture and fisheries, or livelihood
742 conversion. In contrast, inland areas, where the level of salinity intrusion is lower, have less variation in agricultural
743 production models, and communities in these areas still mainly maintain traditional agricultural practices. The
744 findings may indicate that the coping strategies and adaptive capacity of the communities depend on the level of
745 salinity intrusion in the areas. In addition, it can be seen that in areas with high salinity intrusion, people have
746 difficulty in accessing fresh water for agricultural production; therefore, the communities in this area tend to depend
747 more on non-agricultural sources of income. Previous studies– (Nguyen et al., 2019; Yuen et al., 2021) have
748 demonstrated this trend.

Formatted: English (United States)

Formatted: English (United States)

749 The results of the study emphasize that the integration of advanced machine learning models and sociological
750 surveys not only improves the comprehensive research ability from natural factors to socio-economic factors but can
751 also support policymakers and planners to develop appropriate adaptation solutions. Identifying areas affected by
752 saline intrusion by using machine learning models and qualitative analysis of the adaptive capacity of the
753 community is a solid scientific basis for developing policies to minimize the impact of saline intrusion, especially in
754 the context of climate change, to ensure agricultural development and food security.

Formatted: Vietnamese

755 This study was successful in building machine learning models integrated with optimization algorithms to identify
756 the spatial of soil salinity, as well as evaluating farmers' adaptive capacity in the study area. However, in terms of
757 data, this study collected 62 soil salinity samples to build the machine learning model; therefore, the soil salinity
758 map constructed by the proposed models cannot present the trend and drive of soil salinity in time series.
759 Furthermore, soil salinity is significantly affected by climate change and rising sea levels, so it is necessary to assess
760 the effects of this change on soil salinity in the future.

Formatted: Vietnamese

761 As hydrological conditions change, those living in deltas are confronting increased risk. The Red River Delta is one
762 of the largest deltas in the world and, thanks to its fertile floodplains, is home to about 21 million inhabitants. In

Formatted: Vietnamese

763 recent years, in the context of global warming and rising sea levels, these deltas are confronting growing flooding
764 and soil salinity problems, which affect food security in the region and the country. Policies must be implemented to
765 improve the agricultural system and the adaptive capacity of farmers. A proactive approach is required, envisaging
766 multiple scenarios to provide appropriate support for agriculture. These scenarios may include activities and
767 programs adaptive to the different influences of global warming on soil salinity.

768 **6. Conclusion**

769 Soil salinity is a key environmental threat, which will have a growing effect on the development of agriculture and
770 food security globally. A lack of assessment of local adaptive capacities exacerbates the problem. Therefore, this
771 research's objective was to construct a theoretical framework to assess soil salinity and farmers' adaptive capacity
772 based on machine learning, optimization algorithms, remote sensing, and interviews with local people. The results in
773 this study represent a novel contribution to the literature for researchers worldwide and can support policy-makers
774 and farmers to establish suitable strategies to limit damage related to soil salinity. The outcome of this research is as
775 follows.

776 - This study justified the effectiveness of machine learning and remote sensing in soil salinity monitoring in the Red
777 River Delta. The results of this study can be opened to realize in different regions.

778 - Five optimization algorithms, namely POA, STO, SOA, PSO, and GOA, were successful in optimizing the
779 accuracy of the XGB model. All these algorithms were successful in improving the accuracy of XGB. Of these, the
780 XGB-POA model showed the greatest performance, with an R^2 value of 0.968. This was followed by XGB-STO
781 ($R^2=0.967$), XGB-SOA ($R^2=0.966$), XGB-PSO ($R^2=0.964$), and XGB-GOA ($R^2=0.964$).

782 - The models in this research were utilized to construct soil salinity maps. The maps demonstrated that littoral areas
783 and those along the rivers were the most influenced by the soil salinity problem because these regions are influenced
784 by seawater. In addition, when the river levels are lower during the dry season, it creates the conditions for seawater
785 to penetrate the land.

786 - Five factors were analyzed to consider farmers' adaptive capacity: natural capital, human capital, material
787 resources, financial resources, and social capital. The results show that people have awareness and actions in
788 improving their adaptive capacity to increasingly severe saline intrusion; however, there are still many limitations

789 related to lack of awareness and finance. As a recommendation, the participation of multiple stakeholders is
790 required, with a particular emphasis on the role of policies in sustainably and effectively enhancing people's
791 adaptive capacity.

792 The outcome of this research provides key knowledge on the spatial distribution of soil salinity and farmers'
793 adaptive capacity to growing salinization, to support local authorities or farmers in proposing appropriate measures
794 to reduce soil salinity damage. This can complement a theoretical framework in the existing literature on soil salinity
795 management and adaptive capacity.

796 **Statements and Declarations**

797 **Funding**

798 This research is funded by Vietnam National Foundation for Science and Technology Development (NAFOSTED)
799 under grant number 105.08-2023.13

800 **Competing Interests**

801 The authors declare that they have no conflict of interest.

802 **Ethics and consent to participate**

803 Not applicable

804 **Consent for publication**

805 Not applicable

806 **Authors Contributions**

807 **Huu Duy Nguyen:** Conceptualization, Formal analysis, Funding acquisition, Investigation, Methodology,
808 Supervision, Writing – original draft, Writing – review & editing. **Quang-Thanh Bui:** Conceptualization,
809 Formal analysis, Investigation, Methodology, Supervision, Writing – original draft, Writing – review &
810 editing. **Thi Anh Tam Lai:** Data curation. **Duc Dung Tran:** Data curation, Investigation, Writing –
811 original draft, Writing – review & editing. **Dinh Kha Dang:** Data curation, Investigation. **Himan**
812 **Shahabi:** Writing – original draft, Writing – review & editing.

813 **Availability of data and materials**

814 The datasets used and/or analysed during the current study available from the corresponding author on reasonable
815 request

816 **Reference**

- 817 Aksoy, S., Sertel, E., Roscher, R., Tanik, A., Hamzehpour, N., 2024. Assessment of soil salinity using
818 explainable machine learning methods and Landsat 8 images. *International Journal of Applied*
819 *Earth Observation and Geoinformation* 130, 103879.
820 Al-Sarray, N.H.S., Rahebi, J., Demirhan, A., 2024. Detection of DDoS attacks in SDN with Siberian Tiger
821 Optimization algorithm and deep learning.

822 Alamir, N., Kamel, S., Megahed, T.F., Hori, M., Abdelkader, S.M., 2023. Developing hybrid demand
823 response technique for energy management in microgrid based on pelican optimization
824 algorithm. *Electric Power Systems Research* 214, 108905.

825 Asfaw, E., Suryabagavan, K., Argaw, M., 2018. Soil salinity modeling and mapping using remote sensing
826 and GIS: The case of Wonji sugar cane irrigation farm, Ethiopia. *Journal of the Saudi Society of*
827 *Agricultural Sciences* 17(3), 250-258.

828 Bandak, S., Movahedi-Naeini, S.A., Mehri, S., Lotfata, A., 2024. A longitudinal analysis of soil salinity
829 changes using remotely sensed imageries. *Scientific Reports* 14(1), 10383.

830 Bhuyan, M.I., Supit, I., Kumar, U., Mia, S., Ludwig, F., 2024. The significance of farmers' climate change
831 and salinity perceptions for on-farm adaptation strategies in the south-central coast of
832 Bangladesh. *Journal of Agriculture and Food Research* 16, 101097.

833 Bui, D.T., Pradhan, B., Nampak, H., Bui, Q.-T., Tran, Q.-A., Nguyen, Q.-P., 2016. Hybrid artificial
834 intelligence approach based on neural fuzzy inference model and metaheuristic optimization for
835 flood susceptibility modeling in a high-frequency tropical cyclone area using GIS. *Journal of*
836 *Hydrology* 540, 317-330.

837 Castelletti, A., Pianosi, F., Quach, X., Soncini-Sessa, R., 2012. Assessing water reservoirs management
838 and development in Northern Vietnam. *Hydrology and Earth System Sciences* 16(1), 189-199.

839 Cullu, M.A., 2003. Estimation of the effect of soil salinity on crop yield using remote sensing and
840 geographic information system. *Turkish Journal of Agriculture and Forestry* 27(1), 23-28.

841 Dasgupta, S., Laplante, B., Murray, S., Wheeler, D., 2009. Climate change and the future impacts of
842 storm-surge disasters in developing countries. *Center for Global Development Working Paper*
843 (182).

844 Dehghani, M., Trojovský, P., 2022. Serval optimization algorithm: a new bio-inspired approach for
845 solving optimization problems. *Biomimetics* 7(4), 204.

846 Du, L., Tian, S., Zhao, N., Zhang, B., Mu, X., Tang, L., Zheng, X., Li, Y., 2024. Climate and topography
847 regulate the spatial pattern of soil salinization and its effects on shrub community structure in
848 Northwest China. *Journal of Arid Land*, 1-18.

849 Eldeiry, A.A., Garcia, L.A., Reich, R.M., 2008. Soil salinity sampling strategy using spatial modeling
850 techniques, remote sensing, and field data. *Journal of irrigation and drainage engineering*
851 134(6), 768-777.

852 Elshewy, M.A., Mohamed, M.H., Refaat, M., 2024. Developing a soil salinity model from landsat 8
853 satellite bands based on advanced machine learning algorithms. *Journal of the Indian Society of*
854 *Remote Sensing* 52(3), 617-632.

855 Fathizad, H., Ardakani, M.A.H., Sodaiezhadeh, H., Kerry, R., Taghizadeh-Mehrjardi, R., 2020. Investigation
856 of the spatial and temporal variation of soil salinity using random forests in the central desert of
857 Iran. *Geoderma* 365, 114233.

858 Fu, C., Gan, S., Yuan, X., Xiong, H., Tian, A., 2018. Determination of soil salt content using a probability
859 neural network model based on particle swarm optimization in areas affected and non-affected
860 by human activities. *Remote Sensing* 10(9), 1387.

861 Gong, Z., He, H., Fan, D., Sheng, J., Zhang, X., 2023. Inversion of sea surface salinity in Bay of Bengal
862 based on Catboost algorithm, Second International Conference on Geographic Information and
863 Remote Sensing Technology (GIRST 2023). SPIE, pp. 297-304.

864 Hardie, M., Doyle, R., 2012. Measuring soil salinity. *Plant salt tolerance: methods and protocols*, 415-
865 425.

866 He, Y., Yin, H., Chen, Y., Xiang, R., Zhang, Z., Chen, H., 2024. Soil Salinity Estimation based on Sentinel-1/2
867 Texture Features and Machine Learning. *IEEE Sensors Journal*.

868 Hien, N.T., Yen, N.H., Balistocchi, M., Peli, M., Cat, V.M., Ranzi, R., 2023. Salinity dynamics under
869 different water management plans coupled with sea level rise scenarios in the Red River Delta,
870 Vietnam. *Journal of Hydro-environment Research* 51, 67-81.

871 Hoa, P.V., Giang, N.V., Binh, N.A., Hai, L.V.H., Pham, T.-D., Hasanlou, M., Tien Bui, D., 2019. Soil salinity
872 mapping using SAR sentinel-1 data and advanced machine learning algorithms: A case study at
873 Ben Tre Province of the Mekong River Delta (Vietnam). *Remote Sensing* 11(2), 128.

874 Hoang, L.P., Pot, M., Tran, D.D., Ho, L.H., Park, E., 2023. Adaptive capacity of high- and low dyke farmers
875 to hydrological changes in the Vietnamese Mekong delta. *Environmental Research* 224, 115423.

876 Hoang, N.K., Hai, D.T., 2024. Assessing surface water salinity intrusion in the Mekong River Delta: a case
877 study in Rach Gia, Vietnam. *GeoJournal* 89(4), 171.

878 Hung, N.M., Larson, M., 2014. Coastline and river mouth evolution in the central part of the Red River
879 Delta, Coastal disasters and climate change in Vietnam. Elsevier, pp. 43-79.

880 Ingle, K.K., Jatoth, R.K., 2024. Non-linear Channel Equalization using Modified Grasshopper Optimization
881 Algorithm. *Applied Soft Computing* 153, 110091.

882 Jia, P., Zhang, J., Liang, Y., Zhang, S., Jia, K., Zhao, X., 2024. The inversion of arid-coastal cultivated soil
883 salinity using explainable machine learning and Sentinel-2. *Ecological Indicators* 166, 112364.

884 Jiang, H., Rusuli, Y., Amuti, T., He, Q., 2019. Quantitative assessment of soil salinity using multi-source
885 remote sensing data based on the support vector machine and artificial neural network.
886 *International journal of remote sensing* 40(1), 284-306.

887 Juneja, M., Nagar, S., 2016. Particle swarm optimization algorithm and its parameters: A review, 2016
888 International Conference on Control, Computing, Communication and Materials (ICCCCM). IEEE,
889 pp. 1-5.

890 Kaplan, G., Gašparović, M., Alqasemi, A.S., Aldaheri, A., Abuelgasim, A., Ibrahim, M., 2023. Soil salinity
891 prediction using Machine Learning and Sentinel – 2 Remote Sensing Data in Hyper – Arid areas.
892 *Physics and Chemistry of the Earth, Parts A/B/C* 130, 103400.

893 Kennedy, J., Eberhart, R., 1995. Particle swarm optimization, *Proceedings of ICNN'95-international*
894 *conference on neural networks. ieee*, pp. 1942-1948.

895 Le Dang, H., Li, E., Nuberg, I., Bruwer, J., 2014. Understanding farmers' adaptation intention to climate
896 change: A structural equation modelling study in the Mekong Delta, Vietnam. *Environmental*
897 *science & policy* 41, 11-22.

898 Li, S., Zhang, T., Yu, J., 2023. Photovoltaic array dynamic reconfiguration based on an improved pelican
899 optimization algorithm. *Electronics* 12(15), 3317.

900 Liu, W., Chen, Z., Hu, Y., 2022. XGBoost algorithm-based prediction of safety assessment for pipelines.
901 *International Journal of Pressure Vessels and Piping* 197, 104655.

902 Liu, Y., Han, X., Zhu, Y., Li, H., Qian, Y., Wang, K., Ye, M., 2024. Spatial mapping and driving factor
903 Identification for salt-affected soils at continental scale using Machine learning methods. *Journal*
904 *of Hydrology* 639, 131589.

905 Ma, G., Ding, J., Han, L., Zhang, Z., Ran, S., 2021. Digital mapping of soil salinization based on Sentinel-1
906 and Sentinel-2 data combined with machine learning algorithms. *Regional Sustainability* 2(2),
907 177-188.

908 Mazumder, M.S.U., Kabir, M.H., 2022. Farmers' adaptations strategies towards soil salinity effects in
909 agriculture: the interior coast of Bangladesh. *Climate Policy* 22(4), 464-479.

910 Mirjalili, S.Z., Mirjalili, S., Saremi, S., Faris, H., Aljarah, I., 2018. Grasshopper optimization algorithm for
911 multi-objective optimization problems. *Applied Intelligence* 48, 805-820.

912 Mo, H., Sun, H., Liu, J., Wei, S., 2019. Developing window behavior models for residential buildings using
913 XGBoost algorithm. *Energy and Buildings* 205, 109564.

Formatted: French (France)

Formatted: French (France)

914 Moayedi, H., Gör, M., Lyu, Z., Bui, D.T., 2020. Herding Behaviors of grasshopper and Harris hawk for
915 hybridizing the neural network in predicting the soil compression coefficient. *Measurement* 152,
916 107389.

917 Moayedi, H., Nguyen, H., Kok Foong, L., 2021. Nonlinear evolutionary swarm intelligence of grasshopper
918 optimization algorithm and gray wolf optimization for weight adjustment of neural network.
919 *Engineering with Computers* 37(2), 1265-1275.

920 Mukhamediev, R.I., Merembayev, T., Kuchin, Y., Malakhov, D., Zaitseva, E., Levashenko, V., Popova, Y.,
921 Symagulov, A., Sagatdinova, G., Amirgaliyev, Y., 2023. Soil Salinity Estimation for South
922 Kazakhstan Based on SAR Sentinel-1 and Landsat-8, 9 OLI Data with Machine Learning Models.
923 *Remote Sensing* 15(17), 4269.

924 Nguyen, H.D., 2022. Hybrid models based on deep learning neural network and optimization algorithms
925 for the spatial prediction of tropical forest fire susceptibility in Nghe An province, Vietnam.
926 *Geocarto International* 37(26), 11281-11305.

927 Nguyen, H.D., Van, C.P., Nguyen, T.G., Dang, D.K., Pham, T.T.N., Nguyen, Q.-H., Bui, Q.-T., 2023. Soil
928 salinity prediction using hybrid machine learning and remote sensing in Ben Tre province on
929 Vietnam's Mekong River Delta. *Environmental Science and Pollution Research*, 1-18.

930 Nguyen, M.T., Renaud, F.G., Sebesvari, Z., 2019. Drivers of change and adaptation pathways of
931 agricultural systems facing increased salinity intrusion in coastal areas of the Mekong and Red
932 River deltas in Vietnam. *Environmental science & policy* 92, 331-348.

933 Nguyen, P.T., Koedsin, W., McNeil, D., Van, T.P., 2018. Remote sensing techniques to predict salinity
934 intrusion: application for a data-poor area of the coastal Mekong Delta, Vietnam. *International*
935 *journal of remote sensing* 39(20), 6676-6691.

936 Nguyen, Q.H., Takewaka, S., 2020. Land subsidence and its effects on coastal erosion in the Nam Dinh
937 Coast (Vietnam). *Continental Shelf Research* 207, 104227.

938 Nguyen, T.G., Tran, N.A., Vu, P.L., Nguyen, Q.-H., Nguyen, H.D., Bui, Q.-T., 2021. Salinity intrusion
939 prediction using remote sensing and machine learning in data-limited regions: A case study in
940 Vietnam's Mekong Delta. *Geoderma Regional* 27, e00424.

941 Nguyen, V.H., Germer, J., Asch, F., 2024. Evaluating topsoil salinity via geophysical methods in rice
942 production systems in the Vietnam Mekong Delta. *Journal of Agronomy and Crop Science*
943 210(1), e12676.

944 Nguyen, Y.T.B., Kamoshita, A., Dinh, V.T.H., Matsuda, H., Kurokura, H., 2017. Salinity intrusion and rice
945 production in Red River Delta under changing climate conditions. *Paddy and Water Environment*
946 15, 37-48.

947 Nhuan, M.T., Van Ngoi, C., Nghi, T., Tien, D.M., van Weering, T.C., van den Bergh, G., 2007. Sediment
948 distribution and transport at the nearshore zone of the Red River delta, Northern Vietnam.
949 *Journal of Asian Earth Sciences* 29(4), 558-565.

950 Premkumar, N., Santhosh, R., 2024. Pelican optimization algorithm with blockchain for secure load
951 balancing in fog computing. *Multimedia Tools and Applications* 83(18), 53417-53439.

952 Quang, N.H., Viet, T.Q., Thang, H.N., Hieu, N.T.D., 2024. Long-term water level dynamics in the Red River
953 basin in response to anthropogenic activities and climate change. *Science of The Total*
954 *Environment* 912, 168985.

955 Ramraj, S., Uzir, N., Sunil, R., Banerjee, S., 2016. Experimenting XGBoost algorithm for prediction and
956 classification of different datasets. *International Journal of Control Theory and Applications*
957 9(40), 651-662.

958 Rhoades, J., Ingvalson, R., 1971. Determining salinity in field soils with soil resistance measurements. *Soil*
959 *Science Society of America Journal* 35(1), 54-60.

960 Rini, D.P., Shamsuddin, S.M., Yuhaziz, S.S., 2011. Particle swarm optimization: technique, system and
961 challenges. *International journal of computer applications* 14(1), 19-26.

962 Ruidas, D., Chakraborty, R., Islam, A.R.M.T., Saha, A., Pal, S.C., 2022. A novel hybrid of meta-
 963 optimization approach for flash flood-susceptibility assessment in a monsoon-dominated
 964 watershed, Eastern India. *Environmental earth sciences* 81(5), 145.
 965 Shi, H., Hellwich, O., Luo, G., Chen, C., He, H., Ochege, F.U., Van de Voorde, T., Kurban, A., De Maeyer, P.,
 966 2021. A global meta-analysis of soil salinity prediction integrating satellite remote sensing, soil
 967 sampling, and machine learning. *IEEE Transactions on Geoscience and Remote Sensing* 60, 1-15.
 968 Sindi, A.O.N., Si, P., Li, Q., 2024. Secure Task Offloading and Resource Allocation Strategies in Mobile
 969 Applications Using Probit Mish-Gated Recurrent Unit and an Enhanced-Searching-Based Serval
 970 Optimization Algorithm. *Electronics* 13(13), 2462.
 971 Song, Y., Gao, M., Wang, J., 2024. Inversion of salinization in multilayer soils and prediction of water
 972 demand for salt regulation in coastal region. *Agricultural Water Management* 301, 108970.
 973 Su, Y., Li, T., Cheng, S., Wang, X., 2020. Spatial distribution exploration and driving factor identification
 974 for soil salinisation based on geodetector models in coastal area. *Ecological Engineering* 156,
 975 105961.
 976 Tan, J., Ding, J., Han, L., Ge, X., Wang, X., Wang, J., Wang, R., Qin, S., Zhang, Z., Li, Y., 2023. Exploring
 977 planetScope satellite capabilities for soil salinity estimation and mapping in arid regions oases.
 978 *Remote Sensing* 15(4), 1066.
 979 Thiam, H.I., Owusu, V., Villamor, G.B., Schuler, J., Hathie, I., 2024. Farmers' intention to adapt to soil
 980 salinity expansion in Fimela, Sine-Saloum area in Senegal: A structural equation modelling
 981 approach. *Land Use Policy* 137, 106990.
 982 Tran, V.N., Kim, J., 2022. Robust and efficient uncertainty quantification for extreme events that deviate
 983 significantly from the training dataset using polynomial chaos-kriging. *Journal of Hydrology* 609,
 984 127716.
 985 Trojovský, P., Dehghani, M., 2022. Pelican optimization algorithm: A novel nature-inspired algorithm for
 986 engineering applications. *Sensors* 22(3), 855.
 987 Trojovský, P., Dehghani, M., Hanuš, P., 2022. Siberian tiger optimization: A new bio-inspired
 988 metaheuristic algorithm for solving engineering optimization problems. *Ieee Access* 10, 132396-
 989 132431.
 990 Vermeulen, D., Van Niekerk, A., 2017. Machine learning performance for predicting soil salinity using
 991 different combinations of geomorphometric covariates. *Geoderma* 299, 1-12.
 992 Vinh, V.D., Ouillon, S., Thanh, T.D., Chu, L., 2014. Impact of the Hoa Binh dam (Vietnam) on water and
 993 sediment budgets in the Red River basin and delta. *Hydrology and Earth System Sciences* 18(10),
 994 3987-4005.
 995 Wang, H., Hsieh, Y.P., Harwell, M.A., Huang, W., 2007. Modeling soil salinity distribution along
 996 topographic gradients in tidal salt marshes in Atlantic and Gulf coastal regions. *Ecological*
 997 *modelling* 201(3-4), 429-439.
 998 Wang, H., Zhang, L., Zhao, J., Hu, X., Ma, X., 2022. Application of hyperspectral technology combined
 999 with bat algorithm-AdaBoost model in field soil nutrient prediction. *Ieee Access* 10, 100286-
 1000 100299.
 1001 Wang, J., Peng, J., Li, H., Yin, C., Liu, W., Wang, T., Zhang, H., 2021. Soil salinity mapping using machine
 1002 learning algorithms with the Sentinel-2 MSI in arid areas, China. *Remote Sensing* 13(2), 305.
 1003 Wang, J., Wang, X., Zhang, J., Shang, X., Chen, Y., Feng, Y., Tian, B., 2024. Soil Salinity Inversion in Yellow
 1004 River Delta by Regularized Extreme Learning Machine Based on ICOA. *Remote Sensing* 16(9),
 1005 1565.
 1006 Wang, W., Sun, J., 2024. Estimation of soil salinity using satellite-based variables and machine learning
 1007 methods. *Earth Science Informatics*, 1-13.

1008 Wu, W., Zucca, C., Muhaimeed, A.S., Al-Shafie, W.M., Fadhil Al-Quraishi, A.M., Nangia, V., Zhu, M., Liu,
1009 G., 2018. Soil salinity prediction and mapping by machine learning regression in C entral M
1010 esopotamia, I raq. *Land degradation & development* 29(11), 4005-4014.

1011 Xiao, C., Ji, Q., Chen, J., Zhang, F., Li, Y., Fan, J., Hou, X., Yan, F., Wang, H., 2023. Prediction of soil salinity
1012 parameters using machine learning models in an arid region of northwest China. *Computers and*
1013 *Electronics in Agriculture* 204, 107512.

1014 Xiao, S., Nurmemet, I., Zhao, J., 2024. Soil salinity estimation based on machine learning using the GF-3
1015 radar and Landsat-8 data in the Keriya Oasis, Southern Xinjiang, China. *Plant and Soil* 498(1),
1016 451-469.

1017 Xie, J., Shi, C., Liu, Y., Wang, Q., Zhong, Z., Wang, X., He, S., Feature Variable Selection Methods for
1018 Inversion of Soil Salinity at the Irrigation District Scale Based on Machine Learning. Available at
1019 SSRN 4865442.

1020 Yuen, K.W., Hanh, T.T., Quynh, V.D., Switzer, A.D., Teng, P., Lee, J.S.H., 2021. Interacting effects of land-
1021 use change and natural hazards on rice agriculture in the Mekong and Red River deltas in
1022 Vietnam. *Natural Hazards and Earth System Sciences* 21(5), 1473-1493.

1023 Zhang, W., Zhang, W., Liu, Y., Zhang, J., Yang, L., Wang, Z., Mao, Z., Qi, S., Zhang, C., Yin, Z., 2022. The
1024 role of soil salinization in shaping the spatio-temporal patterns of soil organic carbon stock.
1025 *Remote Sensing* 14(13), 3204.

1026 Zhao, R., Ni, H., Feng, H., Song, Y., Zhu, X., 2019. An improved grasshopper optimization algorithm for
1027 task scheduling problems. *Int. J. Innov. Comput., Inf. Control* 15, 1967-1987.

1028

1029